Pharmacokinetics of IV LMP744, a Novel Topoisomerase 1 Inhibitor, in Humans

by

Joshua J. Deppas

Bachelor of Science (B.S.) Indiana University of Pennsylvania, 2016

Submitted to the Graduate Faculty of

The School of Pharmacy in partial fulfillment

of the requirements for the degree of

Master of Science

University of Pittsburgh

2020

UNIVERSITY OF PITTSBURGH

SCHOOL OF PHARMACY

This thesis was presented

by

Joshua J. Deppas

It was defended on

August 10, 2020

and approved by

Lisa Rohan, Ph.D., Dept. of Pharmaceutical Sciences

Raman Venkataramanan, Ph.D., Dept. of Pharmaceutical Sciences

Thesis Advisor: Jan H. Beumer, Pharm.D. Ph.D., D.A.B.T., Dept. of Pharmaceutical Sciences

Pharmacokinetics of IV LMP744, a Novel Topoisomerase 1 Inhibitor, in Humans

Joshua J. Deppas

University of Pittsburgh, 2020

During transcription and replication, DNA is supercoiled creating tension and strain downstream of the replication site. To relax supercoiling, DNA topoisomerase 1 (TOP1) generates temporary DNA single-strand breaks resulting in the cleaved strands ability to rotate freely around the DNA double helix, thereby relieving strain. TOP1, which is responsible for genetic recombination and religation of cleaved DNA, is overexpressed in tumor cells and ultimately results in an intact DNA duplex. Pharmacological TOP1 inhibitors prevent tension relief and religation ultimately resulting in lethal DNA strand breaks leading to cell death.

Consequently, TOP1 is a clinically proven target for the management and treatment of various cancers in humans. Currently, the FDA has approved two analogue TOP1 inhibitors, topotecan and irinotecan, that are derived from a less potent predecessor, camptothecins. The clinical drawbacks of camptothecin analogs, include chemical instability, short half-lives and common dose-limiting adverse events. These limitations have resulted in the discovery and development of the indenoisoquinolines, a non-camptothecin family of TOP1 inhibitors. Of these derivatives, LMP744 has been identified as a possible therapeutic and is being investigated clinically.

To support clinical development of LMP744, plasma samples were collected and concentration-time data was generated using two LC-MS/MS assays. Data was collected from 17 different patients who received intravenous infusions of LMP744 ranging from 6 to 190 mg/m^2.

Noncompartmental and compartmental analyses were performed to obtain LMP744 pharmacokinetic parameters and to evaluate dose linearity. The effect of BSA and body weight on the clearance and volume of distribution of LMP744 were also evaluated. The data presented here will hopefully support the development of this drug that is currently in clinical trials conducted to identify the safety, tolerability, optimal dose, and efficacy of LMP744 in cancer patients.

TABLE OF CONTENTS

1.0 INTRODUCTION 13

1.1 DNA REPLICATION AND SUPERCOILING 13

1.1.1 Topoisomerase Enzymes 13

1.1.2 TOP1 as a Target in Cancer Therapy 14

1.2 NONCLINICAL STUDIES 16

1.3 DOSE LINEARITY AND BSA BASED DOSING 19

1.4 EVALUATION OF LMP744 PHARMACOKINETICS 21

2.0 MATERIALS AND METHODS 22

2.1 CHEMICALS AND SOLVENTS 22

2.2 VALIDATED LC-MS/MS METHOD 23

2.2.1 Sample Preparation 24

2.3 NOVEL, MORE SENSITIVE LC-MS/MS METHOD 25

2.3.1 Sample Preparation 27

2.4 IMPLEMENTATION AND VALIDATION 27

2.5 PHARMACOKINETICS 28

2.5.1 Noncompartmental Analysis of LMP744 28

2.5.2 Compartmental Modeling of LMP744 29

2.5.3 Comparison of NCA and Compartmental Modeling 31

2.6 DOSE LINEARITY 31

2.7 BSA AND WEIGHT AS COVARIATES 32

2.7.1 BSA as a Covariate on Clearance 32

2.7.2 Weight as a Covariate on Distribution Volume 32
3.0 RESULTS 34
3.1 QUANTITATIVE LC-MS/MS ASSAYS 34
3.1.1 Assay Comparison 34
3.1.2 Cross-Validation 38
3.2 PHARMACOKINETICS 40
3.2.1 Noncompartmental Modeling Analysis 44
3.2.2 Compartmental Modeling 47
3.2.3 Comparison of NCA and Compartmental Modeling 48
3.3 DOSE LINEARITY OF LMP744 50
3.3.1 Dose Normalization 51
3.3.2 Log-Normal Transformation 53
3.4 BSA AND WEIGHT AS COVARIATES 56
3.4.1 BSA as a Covariate on Clearance 57
3.4.2 Weight as a Covariate on Distribution Volume 59
4.0 DISCUSSION 62
5.0 CONCLUSIONS AND FUTURE DIRECTIONS 67
BIBLIOGRAPHY 68

LIST OF TABLES

Table 1. Patient specific weight (kg), dose (mg/m^2), BSA (m^2), and absolute dose (mg) administered to all patients 29

Table 2. Assay performance data of the calibration samples of LMP744 in human plasma using the validated assay. Standard calibrators were run in triplicate and average concentration values were taken. QCs were run in duplicate and average concentration values were used. 36

Table 3. Assay performance data of the calibration samples of LMP744 in human plasma using the, more sensitive, assay. Standard calibrators were run in triplicate and average concentration values were taken. QCs were run in duplicate and average concentration values were used. 38

Table 4. Demographics of patients receiving a daily infusion of LMP744 40

Table 5. Noncompartmental AUC parameters of LMP744 in humans derived from the first 24 h 46

Table 6. Remaining PK parameters of LMP744 in humans derived with NCA 47

Table 7. Plasma PK parameters and R^2 values derived from 2-compartmental modeling analysis of LMP744 in humans. 48

Table 8. Comparison of clearance, volume of distribution and half-life values derived by NCA relative to compartmental modeling. 49

Table 9. Dose normalized C_{max} and AUC values of LMP744 administered in humans 51

Table 10. Log-normalized absolute dosages, C_{max} and AUC values of LMP744 in humans 54

Table 11. BSA-normalized clearance and weight-normalized volume of distribution values for patients administered LMP744 as derived with compartmental modeling. 57

Table 12. Total clearance of LMP744 normalized by the average patient clearance from compartmental analysis and BSA normalized clearance values normalized by its mean. 58

Table 13. Statistical results from F-test showing a lack of significant difference between variances of LMP744 clearance and BSA-normalized LMP744 clearance in humans. 59

Table 14. Volume of distribution of LMP744 normalized by the average volume of distribution and volume of distribution normalized by patient weight normalized by the average. 60

Table 15. Statistical results from F-test showing a lack of statistical significance between weight and volume of distribution of LMP744 in humans. 61

LIST OF FIGURES

Figure 1. Relaxation of DNA supercoiling via TOPcc [5] 14

Figure 2. Structure of topotecan. 18

Figure 3. Structure of irinotecan 18

Figure 4. Structure of LMP744 18

Figure 5. Elution pattern of internal standards. In order of elution: acetaminophen (1.2 min), veliparib (1.8 min), busulfan (2.5 min), neratinib (3 min), erlotinib (3.6 min), abiraterone (4.4 min), bicalutamide (4.8 min) and paclitaxel (5.1 min). 26

Figure 6. A simplified 2-compartment model showing drug absorbed into the first compartment via IV injection, with distribution and redistribution to and from a peripheral compartment followed by elimination of the drug from the central compartment 30

Figure 7. Average concentration values from a triplicate standard curve of LMP744 quantified using the validated LC-MS/MS assay, showing linearity over a concentration range of 10-3000 ng/mL with an R^2 value of 0.999. 35

Figure 8. Average concentration values from a triplicate standard curve of LMP744 quantified using the novel, more sensitive, assay, showing linearity over a concentration range of 1-300 ng/mL with an R^2 value of 0.999 37

Figure 9. Concentrations deviations between drug concentrations originally calculated from the validated LC-MS/MS and the novel, more sensitive, assay, shown as percentages. 39

Figure 10. Deviations on a per-patient basis comparing drug concentrations originally calculated from the validated LC-MS/MS and the novel, more sensitive, assay, shown as percentages 39

Figure 11. Concentration vs time results from 1 patient receiving daily 1 hour infusions of LMP744 for 5 days at the dosing level of 6 mg/m^2 41

Figure 12. Concentration vs time results from 1 patient receiving daily 1 hour infusions of LMP744 for 5 days at the dosing level of 12 mg/m^2 41

Figure 13. Concentration vs time results from 3 patients receiving daily 1 hour infusions of LMP744 for 5 days at the dosing level of 24 mg/m^2 42

Figure 14. Concentration vs time results from 2 patients receiving daily 1 hour infusions of LMP744 for 5 days at the dosing level of 48 mg/m^2 42

Figure 15. Concentration vs time results from 9 patients receiving daily 1 hour infusions of LMP744 for 5 days at the dosing level of 190 mg/m^2 43

Figure 16. Concentration vs time results form 1 patient receiving daily 1 hour infusions of LMP744 for 5 days at the dosing level of 260 mg/m^2 43

Figure 17. Amount of the LMP744 administered dose recovered in urine from each patient..... 44

Figure 18. Dose normalized C_{max} concentrations vs absolute dose of administered LMP744 52

Figure 19. Dose normalized AUC values vs absolute dose of administered LMP744 52

Figure 20. Log-normal C_{max} vs log-normal absolute dose of LMP744 55

Figure 21. Log-normal AUC vs log-normal absolute dose of LMP744 55

LIST OF EQUATIONS

Equation 1. Power model equation for formal dose linearity [24] 19

Equation 2. Logarithmic transformation of the power model [24]..... 20

Equation 3. Equation for AUC 30

Equation 4. Equation for comparing PK parameters calculated from NCA and compartmental modeling 31

Equation 5. Equation for extrapolated AUC 44

1.0 INTRODUCTION

1.1 DNA REPLICATION AND SUPERCOILING

The double helix structure of DNA not only provides a foundation for the continuous duplication and decoding of genetic material, but also acts as a safeguard for DNA strand integrity. Hydrogen bonds help to stabilize the two interweaving and complementary single-stranded polynucleotide strands. However, these properties also cause spatial constraints during DNA replication [1-4]. If these constraints are not promptly relaxed, or chemically inhibited, overwound DNA is generated [4]. Specifically, during DNA replication each single strand of DNA serves as a corresponding template for polymerization of the complementary single strand. Eventually, this progressive sequence of unwinding DNA strands causes over winding, or supercoiling, tension distal to the replication fork [4].

1.1.1 Topoisomerase Enzymes

The ability of cells to overcome DNA supercoiling while separating DNA molecules is crucial for replication, gene expression and chromosomal segregation. It is also very important for this process to occur while simultaneously maintaining chromosomal integrity. Specialized enzymes known as topoisomerases overcome these barriers by catalyzing modifications in the DNA helices by cutting, or "nicking" one or both strands of the double helix. These transient induced breaks are referred to as topoisomerase cleavage complexes (TOPcc). Following TOPcc formation, the DNA strand is then passed through the break(s) thereby changing the overall DNA

topology and alleviating tension caused by replication induced supercoiling. The breaks are then closed via DNA reformation of the original phosphodiester-bond followed by enzyme release from the complex. Type 1 topoisomerases (TOP1) change the degree of supercoiling of DNA by causing single-strand breaks and religation, whereas type 2 topoisomerases (TOP2) initiate double-strand breaks to alleviate tension. A simplified TOP1 mechanism can be seen in **Figure 1**.

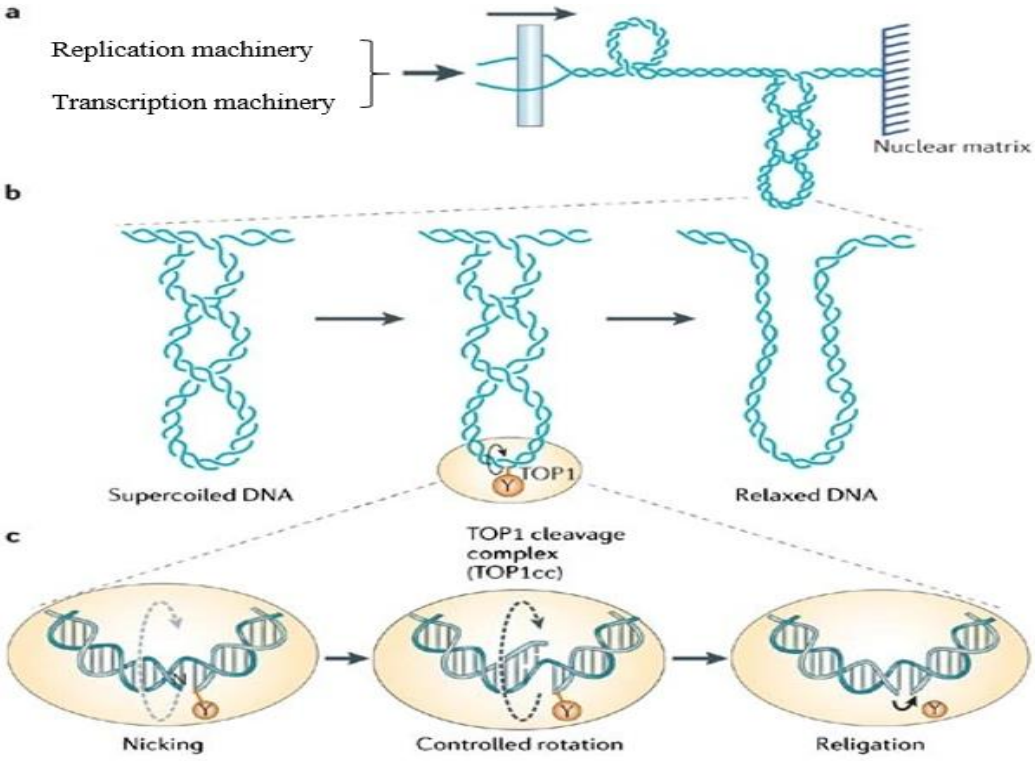

Figure 1. Relaxation of DNA supercoiling via TOPcc [5]

1.1.2 TOP1 as a Target in Cancer Therapy

Among topoisomerase DNA-targeted therapies, TOP1 inhibitors topotecan (**Figure 2**) and irontecan (**Figure 3**) are widely used in a broad range of tumors as late-stage therapy either alone or in combination therapies [6-12]. However, these camptothecin (CPT) based therapies are the

only chemical class of TOP1 inhibitors currently approved by the FDA. Though these treatments have well documented advantages, CPT-based TOP1 inihbitors have several limititations as well [5, 11]. These limititations include chemical instability, a short plasma half-life due to rapid elimiation, reversible DNA damage, gastrointestinal (GI) toxicities, and dose-limiting bone marrow toxicities [5, 13-16]. To address these issues, the National Cancer Institute (NCI) has led investigations that have resulted in the identification of a novel class of TOP1 inhibitors: known as indenoisoquinolines [17]. Indenoisoquinolines act as "interfacial inhibitors" and under normal conditions shift the equilibrium to favor DNA cleavage as opposed to DNA religation [18]. Indenoisoquinolines, or non-CPT, based drugs have been shown to overcome most of the limitations caused by camptochecins and are chemically stable, have a longer plasma half-life with no GI irritability, and inhibit TOP1 even after removal of drug [5, 16, 19]. LMP744 (**Figure 4**) is a indenoisoquinoline derivative and TOP1 inhibitor. LMP744 binds to and stabilizes TOPcc ultimately preventing DNA religation thereby inducing irrereversible DNA strand breaks which then leads to cellular apoptosis, tumor shrinkage, and extended patient survival [20-22]. LMP744 has been shown to induce more stable TOP1cc compared to those of the CPT derivatives [23]. This could be advantages to cancer therapy because the rapid reversibility of TOPcc induced from CPT administration requires long drug infusions. In addition, the CPT derivative irinotecan must be bioactivated via hydrolysis to its active metabolite, SN-38. For LMP744, metabolic activation is not required for therapeutic benefit. Additionally, LMP744 has been shown to have a two times faster TOPcc rate constant than for CPT. Suggesting that LMP744 may enhance and strengthen TOPcc formation in cancer patients. Furthermore, LMP744 has been shown to induce TOPcc while in the biological presence of CPT-resistant TOP1 enzymes. However, LMP744 is not a DNA intercalator and has not shown evidence to unwind DNA in the absence of TOP1 [18]. Ultimately,

LMP744 has been shown to inhibit TOP1 mediated DNA relaxation and TOPcc induced by LMP744 are more persistent upon drug removal than those induced by CPT derivatives.

1.2 NONCLINICAL STUDIES

In the NCI160 cell line *in vitro* screen, LMP744 demonstrated modest growth inhibition in several mouse xenograft models. In nude mice bearing human A253 or FaDu head and neck xenografts, LMP744 was found to be moderately active with no significant toxicity. In this study, maximum tumor growth inhibition was 71.8% in the A253 and 69% in the FaDu xenografts after a dose of 50 mg/kg/dose administered once a week for a total of 4 weeks [23]. Antitumor activity was also observed utilizing LMP744 in dogs with lymphoma. In this study, tumor shrinkage was observed in most dogs with an overall response rate of 80%. However, the response rate was not long-lasting and most dogs treated with LMP744 relapsed. Single dose pharmacokinetic (PK) and tissue distribution of LMP744 was assessed in CD2F1 mice following intravenous (IV) and oral (PO) administration. Plasma and tissue samples were collected over the span of 5 minutes to 48 hours post-dose. PK parameters determined from this study included LMP744 having an elimination half-life of 21.1 h, clearance of 0.2 L/hr, AUC of 4824.3 mcg/mL*h, and a steady state volume of distribution of 3.1 L. Dose range-finding toxicity studies were conducted in both rats and dogs. In these studies, toxicity profiles were generated from IV bolus, 1 hour infusion once a day for 5 days. The maximum tolerated dose in rats determined to be > 10mg/kg/day. The recommended first-human dose from the dog studies determined to be 0.16 mg/kg/day as a 1 hour infusion for 5 consecutive days.

To date, the pathway(s) by which LMP744 is eliminated are unknown. For therapeutic use, strong inhibitors and inducers of all major drug metabolizing enzymes and drug transporters are to be avoided while receiving LMP744. Currently, there is no information to suggest any expected differences in drug metabolism, clearance or antitumor effect in one ethnic population compared to another. However, LMP744 has been shown to be a substrate for the ATP-binding cassette transporter protein, ABCG2, or breast cancer resistance protein (BCRP) and p-glycoprotein (P-gP). Therefore, unless medically necessary the use of strong inhibitors and inducers of these transporters should be avoided.

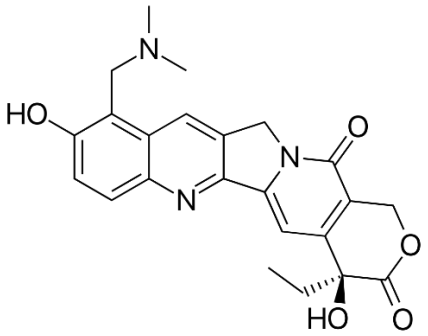

Figure 2. Structure of topotecan.

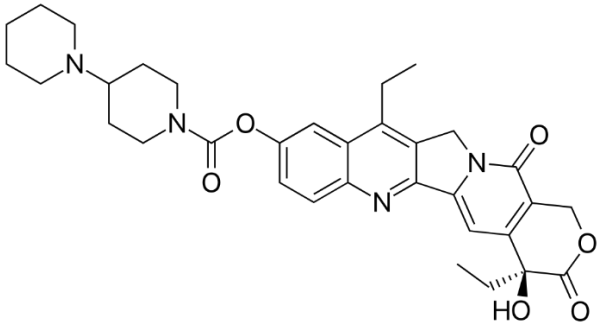

Figure 3. Structure of irinotecan

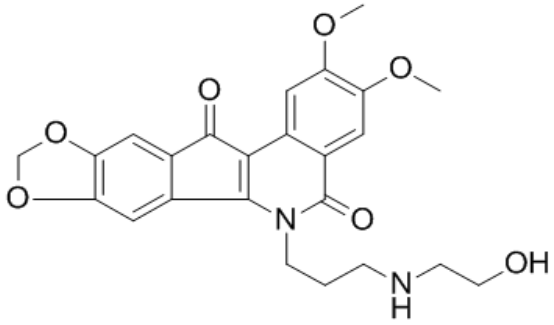

Figure 4. Structure of LMP744

1.3 DOSE LINEARITY AND BSA BASED DOSING

During new drug development, a desirable objective is to identify whether or not the new drug candidate displays linear pharmacokinetic profiles or dose independent PK properties. Doing so helps facilitate proper dosing and dosing regimens in patients receiving the specific treatment. It is therefore vital to identify if the exposure to new drugs are dose proportional or not. Drugs that exhibit nonlinear PK profiles, at expected therapeutic concentration ranges only, will often require additional clinical trials to assess dosing limitations. In order to test dose linearity in humans, a common clinical trial design used is known as a phase 1 dose escalation study. Phase 1 trails provide essential data for furthering the development of anticancer drugs. The key principal in dose escalation studies however is to avoid exposing too many patients to subtherapeutic doses while also maintaining safety by limiting toxicities [21]. Dose linearity occurs when increases in the dose being administered is accompanied by a proportional increase in the systemic exposure of that drug. Doing so, allows for the accurate prediction of systemic concentrations for any given dose within the thereapuetic window (i.e. doubling the dose, will double exposure). Determination of dose proportionality aids in control over the safety and toxicity of a therapeutic. For instance, nonlinear elimination of an administered drug could lead ot unwanted accumulation of systemic concentrations which could have a direct effect on toxicity and efficacy across the dose range. Dose linearity can be observed visually as well as defined when using the power model, originally proposed by Gough *et al,* as seen in the following equation:

$$y = \alpha dose^{\beta}$$

Equation 1. Power model equation for formal dose linearity [24]

This suggests that the relationship between a specifc exposure PK parameter (y) and dose become linear following a logarithemic transformation, to which the following linear regression model can be used:

$$\ln(y) = \mu + \beta \ln(\text{dose})$$

Equation 2. Logarithmic transformation of the power model [24]

Assuming linearity between log(*y*) and log(dose), a value of "β = 1" would indicate perfect linearity between dose and the PK paramter of interest (*y*). Furthermore, an appropriate estimate for β, along with the correct confidence intervals can be used together to identify dose linearity. FDA guidelines for these confidence intervals (CI) have a lower value of: $\vartheta_L = 0.8$ and upper value of: $\vartheta_H = 1.25$ [22]. However, Hummell *et al* suggest this criterion to be impractically strict when applied over an entire dose range, suggesting that more appropriate values for lower and upper limits should be 0.5 and 2.0 for ϑ_L and ϑ_H respectively for exploratory dosing assessments, such as dose escalation studies [24]. To further evaluate how a new drug will interact in humans, body surface area (BSA) based dosing was also studied. Dosing based on a specific patient's BSA is aimed at mitigating variation in exposure, which implicitly assumes that patients with a higher BSA also have a higher clearance and therefore need a higher dose. Clearance has also been shown to correlate with BSA across species. Despite the lack of rigorous studies to prove the validation of BSA-based dosing, it is commonly used for dosing of chemotherapeutic agents [25, 26].

1.4 EVALUATION OF LMP744 PHARMACOKINETICS

There is currently only one type of topoisomerase 1 inhibitor, camptothecins, approved by the FDA for use in humans to treat a variety of cancers. Major drawbacks to camptothecin administration include severe adverse side effects such as diarrhea, nausea, vomiting and overall weakness [27]. Indenoisoquinolines, such as LMP744, possess a structural improvement over camptothecin and its derivatives [28, 29]. They have better chemical stability while producing more stable DNA strand breaks resistant to reversal, and at unique DNA sequences. Additionally, indenoisoquinolines have shown activity against CPT-resistant cell lines [28]. Based on the promising nonclinical data, LMP744 was chosen as a candidate for clinical trials to evaluate its safety, pharmacokinetics and pharmacodynamic profile in cancer patients with refractory solid tumors. This present investigation aimed to identify PK of the novel indenoisoquinoline, non-camptothecin, topoisomerase 1 inhibitor, LMP744. In an effort to describe PK, two separate LC-MS/MS assays were utilized to quantitate drug concentrations in patients who received a daily one-hour infusion of LMP744 over the course of 5 days. Pharmacokinetic parameters were analyzed both noncompartmentally and compartmentally. The effect of BSA and body weight on the clearance and volume of distribution of LMP744 were also evaluated. The data presented here will support the development of this drug that is currently in clinical trials conducted to identify the safety, tolerability, optimal dose, and efficacy of LMP744 in cancer patients.

2.0 MATERIALS AND METHODS

Pharmacokinetic data for this study was generated from plasma samples collected from 17 human patients from a single phase 1 study investigating safety, tolerability and the maximum tolerated dose of LMP744 administered intravenously daily for 5 days (QD x 5) in patients with refractory solid tumors and lymphomas (NCT03030417). The study design was a standard 3+3 dose escalation which began with an accelerated phase. For this type of study, the accelerated phase of dose escalation ends and changes to a standard 3+3 design when one patient experiences dose limiting toxicities. Samples for PK analyses were collected prior to LMP744 administration, then approximately 2 minutes before the end of infusion (EOI) and at approximate time points post infusion. The time points post infusion were as follows: 15 min, 30 min, 1, 2, 4 and 6 hours on day 1. Day 2, 24 h post day 1 start of infusion (SOI) and 2 minutes before EOI. Day 3, 24 h post day 2 SOI and 2 minutes before EOI. Day 4, 24 h post day 3 SOI and 2 minutes before EOI. Day 5, 24 h post day 4 SOI and 2 minutes before EOI and day 8, 72 h post day 5 SOI.

2.1 CHEMICALS AND SOLVENTS

The compound LMP744 (NSC 706744) and isotopic internal standard, [D_4]-LMP744 ([D_4]-NSC 706744), were provided by the National Cancer Institute (Bethesda, MD). Paclitaxel and erlotinib were purchased from LC Labs (Woburn, MA). Acetaminophen, busulfan formic acid, were purchased from Sigma-Aldrich (St. Louis, MO). Abiraterone, neratinib and bicalutamide were purchased from Toronto Research Chemicals (Ontario, Canada). Veliparib was purchased

from Alsachim (Graffenstaden, France). Acetonitrile, ethyl acetate and water (all HPLC grade) were purchased from Fisher Scientific (Fairlawn, NJ). Control heparinized human plasma was purchased from Lampire Biological Laboratories, Inc (Pipersville, PA). Nitrogen needed for sample preparation was purchased from Valley National Gases, Inc. (Pittsburgh, PA)

2.2 VALIDATED LC-MS/MS METHOD

To quantitate drug concentrations in human plasma, a previously validated LC-MS/MS assay was utilized. The deuterated stable isotope labeled [D_4]-LMP744 was used as the internal standard, due to identical physiochemical characteristics to LMP744. The high-performance liquid chromatography (HPLC) system consisted of an Agilent 1100 series autosampler and 1100 series binary pump (Palo Alto, CA). A Phenomenex (Torrance, CA) Synergi Polar-RP 80A (4 µm, 100 x 2 mm) LC column was used for chromatographic separation at 4° C. The solvent for mobile phase A (organic) was 0.1% (*v/v*) formic acid in acetonitrile whereas the mobile phase solvent B (aqueous) was 0.1% (*v/v*) formic acid in water. Initial starting conditions for the assay were a composition of 60% solvent B pumped at a rate of 0.2 mL/min for 4.0 min, changed to 0% solvent B with a flow rate of 0.4 ml/min and held constant for 4.0 minutes. At 8.1 min the percentage of solvent B reverted to initial conditions with a higher flow rate of 0.5 mL/min and allowed to equilibrate for 6.0 min followed by injection of the next sample. Total runtime for this assay was 14 minutes per sample. The retention times (RT) for the parent LMP744 and internal standard D_4-LMP744 were 2.8 and 2.9 min, respectively. The minor differences in RT can be attributed to the 4 deuteriums on the internal standard. which caused a slightly different interaction with the stationary phase of the column.

Mass spectrometric (MS) detection was accomplished utilizing a Waters Quattro Micro mass spectrometer (Milford, Massachusetts) to monitor for *m/z* 453.5 > 392.0 for LMP744 and *m/z* 457.5 > 392.0 for the internal standard. The calibration curve had a linear range of 10 to 3000 ng/mL (10, 30, 100, 300, 600, 1000, 2000, 3000) and samples were prepared in control heparin anticoagulated human plasma. Calibrators were prepared in 0.1% (*v/v*) formic acid in water from serial dilutions of LMP744 in DMSO from a 1.0 mg/mL stock solution stored at -80° C. Quality control (QC) samples were prepared in bulk using control heparin anticoagulated human plasma prior to sample analysis at three different concentration levels: low (25 ng/mL), mid (200ng/mL), and high (2500 ng/mL). QCs were aliquoted to 200 µL and stored at -80° C. On the day of sample analysis, two QCs at each concentration level were analyzed alongside patient samples. A linear $1/y^2$ weighted regression curve was fit to the response ratios vs nominal concentration values of the calibration samples for validity of each run.

2.2.1 Sample Preparation

The sample volume used for this assay was 200 µL of human plasma. All samples were spiked with 10 µL of internal standard solution (D_4-LMP744). Extraction and protein precipitation were done by adding 1 mL ethyl acetate to each sample. Next, samples were vortexed on full speed using a Vortex Genie 2 (Scientific Industries, Bohemia, NY) for one minute and centrifuged using a PrismR microcentrifuge (Labnet International, Inc., Edison, NJ) at 14,000 x g at ambient temperature for 5 minutes. Supernatants were then transferred to borosilicate glass tubes and placed in an evaporation apparatus (Multivap Nitrogen Evaporator, Organomation Associates, Berlin, MA) and allowed to evaporate under a gentle stream of nitrogen gas (Valley National Gases, Inc., Pittsburgh, PA). The process for samples to evaporate properly under the nitrogen

stream took up to 25 minutes. Next, samples were reconstituted in 100 µL of acetonitrile: water: formic acid (50:50:01 *v/v/v*), transferred to microcentrifuge tubes, vortexed and centrifuged again for 3 minutes. This supernatant was loaded into auto-sampler vials, capped and injected (3 µL) in the LC-MS/MS system.

2.3 NOVEL, MORE SENSITIVE LC-MS/MS METHOD

Plasma samples from patients treated at lower LMP744 doses often contained LMP744 concentrations below the lower limit of quantitation (LLOQ) of the FDA guidance validated assay. Therefore, in addition to the validated LC-MS/MS approach (see section 2.2), a more sensitive novel generic assay was needed for the quantitative analysis of drug concentrations in human plasma. This particular assay offers 8 different compounds, which cover a range of polarity, size and ionization that elute over a range of different chromatographic retention times, as a potential internal standard for quantitation of the analyte. The 8 compounds dissolved in the internal standard mix were busulfan, neratinib, erlotinib, veliparib, acetaminophen, bicalutamide, paclitaxel and abiraterone. The elution pattern of internal standards can be seen **Figure 5**. All stock solutions for internal standard use were prepared separately at 1 mg/mL. Stock solutions were prepared as follows: busulfan, neratinib, erlotinib and veliparib were all dissolved in acetonitrile. Acetaminophen was dissolved in methanol. Bicalutamide, paclitaxel and abiraterone were dissolved in DMSO. The compounds were then added to acetonitrile at the following concentrations (ng/mL): busulfan 1000, neratinib 400, erlotinib 5, veliparib 10, acetaminophen 400, bicalutamide 400, paclitaxel 400, and abiraterone 500. Erlotinib was chosen as the internal standard for this assay due to a similar retention time of the desired analyte, LMP744.

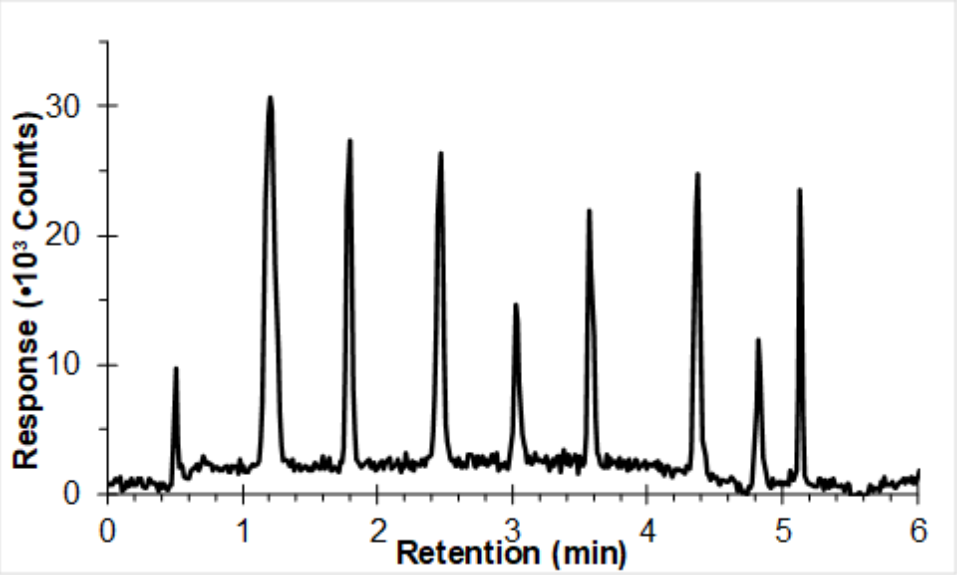

Figure 5. Elution pattern of internal standards. In order of elution: acetaminophen (1.2 min), veliparib (1.8 min), busulfan (2.5 min), neratinib (3 min), erlotinib (3.6 min), abiraterone (4.4 min), bicalutamide (4.8 min) and paclitaxel (5.1 min).

The LC system and mass spectrometer differed from the FDA guidance validated assay, which allowed for greater sensitivity at lower levels of concentration. The LC system consisted of an Agilent (Santa Clara, CA) 1200 SL autosampler and binary pump. The same column and mobile phase from the validated LC-MS/MS approach (see section 2.2) were used for chromatographic separation; however, the mobile phase gradient differed. Initial mobile phase composition started at 95% solvent B pumped at a rate of 0.4 mL/min and decreased in a linear fashion to 5% solvent B over the course of 5 min and held constant for another min. At 6.1 min, solvent B increased back to initial conditions for 2 min, followed by next sample injection. Total run time for this assay was 8 min per sample. The retention times (RT) for the parent LMP744 and internal standard erlotinib were 3.0 and 3.6 min, respectively.

MS detection was done using an ABI SCIEX (Ontario, Canada) 4000Q hybrid linear ion trap tandem mass spectrometer in positive multiple reaction monitoring (MRM) mode. To allow

for a more sensitive quantitative approach, a calibration curve of 1.0 to 300 ng/mL (1, 3, 10, 30, 100, 300) was prepared in control heparin anticoagulated human plasma. Calibrators and QCs were prepared in the same fashion as the above approach (see section 2.2). To adjust for the lowered concentration range, the QC concentration levels were as follows: low (2.5 ng/mL), mid (25 ng/mL) and high (250 ng/mL). Two sets of QCs at each concentration level were analyzed with every run and a linear $1/y^2$ weighted regression curve was fit to the response vs nominal concentration values of the calibration samples for validity of each run.

2.3.1 Sample Preparation

The sample volume used for this assay was 50 µL human plasma which was pipetted into a singular well of an Agilent 31 mm deep 96 well plate (Santa Clara, CA). Next, 150 µL of the erlotinib-internal standard mix was added to each well. The well plate was then vortexed for 1 min on a Vortex Genie 2 set at "4." The well plate was then placed in a Model 5810 R Eppendorf (New York, USA) centrifuge at 2,500 x g at ambient temperature for 10 min. Following separation, a volume of 125 µL of the resultant supernatant was then transferred to a new, clean Agilent 31 mm deep 96 well plate. 500 µL of water was added to each well and the plate was vortexed once more for 10 seconds on a Vortex Genie 2 set at "4." The well plate was then loaded onto the autosampler and 5 µL of each sample was injected in the LC-MS/MS system.

2.4 IMPLEMENTATION AND VALIDATION

The novel, more sensitive, assay was implemented for this study in order to quantitate plasma drug concentrations in the first six patients which had plasma samples with LMP744

concentrations that fell below the LLOQ of the original validated LC-MS/MS method. In addition, samples that were within the original calibration curve were also ran and analyzed with this method. This process allowed for the correct and precise quantitation of plasma drug concentrations at low levels, while also providing a way of cross-validating samples that were previously in range. For cross-validation, we calculated the percent of deviation of values derived with the novel, more sensitive, method from values generated with the validated method.

2.5 PHARMACOKINETICS

2.5.1 Noncompartmental Analysis of LMP744

To evaluate exposure of LMP744 in human plasma, noncompartmental analysis (NCA) was performed using PK Solutions (Summit PK, Montrose, CO). PK parameters C_{max}, T_{max}, AUC_{0-t}, $AUC_{0-\infty}$, $t_{1/2}$, V_d, V_{ss} and Cl were calculated for each patient. C_{max} refers to maximum observed concentration and T_{max} refers the time where the maximum concentration was observed. AUC_{0-t} is defined as the area under the curve from time 0 to the last measurable concentration, which was 24 h, as at that point, the day 2 infusion was started. $AUC_{0-\infty}$ is the area under the curve from time 0 that is extrapolated to infinite time. $T_{1/2}$ refers to the time taken for half of the initial dose to be eliminated from the body (i.e. half-life). V_d refers to the estimated volume that is necessary to contain the amount of administered drug. V_{ss} is defined as the volume of distribution at steady state and Cl refers to the volume of plasma being cleared of LMP744 per unit time (i.e. L/h). Patient-specific absolute dosage (BSA * (dose/mg/m^2) and concentration vs time values through the first

24 hours were used for NCA to ensure only one dose of LMP744 was being evaluated. These patient-specific dose and BSA can be found in **Table 1**.

Table 1. Patient specific weight (kg), dose (mg/m^2), BSA (m^2), and absolute dose (mg) administered to all patients

PT #	Weight kg	Dose mg/m^2	BSA m^2	Absolute Dose mg
1	113.8	6	2.38	14.28
2	96.3	12	1.96	23.52
3	87.3	24	2.06	49.44
4	97.3	24	2.17	52.08
5	105.0	24	2.05	49.20
6	87.0	48	2.03	97.44
7	47.1	96	1.40	134.0
8	124.5	190	2.48	476.2
9	134.5	190	2.69	516.5
10	68.9	190	1.77	336.3
11	9..4	190	2.06	391.4
12	70.5	190	1.90	361.0
13	182.2	190	2.35	446.5
14	100.1	190	2.07	393.3
15	90.1	190	2.07	393.3
16	87.3	190	1.92	364.8
17	50.3	260	1.52	395.20

2.5.2 Compartmental Modeling of LMP744

In addition to NCA, a 2-compartmental modeling approach was used to provide a more accurate representation of the true exposure of LMP744 in human plasma. Compartmental analysis was done using ADAPT 5 (University of Southern California, Los Angeles, CA). Primary PK parameters provided through this model were: CL_t, Cl_d, V_c, V_p, and $t_{1/2}$. CL_t refers to the absolute

or total clearance of LMP744, whereas Cl_d is the distributional clearance. V_c is the central volume of distribution and V_p represents the peripheral volume of distribution. A simplified representation of a 2-compartmental IV model can be seen in **Figure 6**. Infusion rates were calculated (mg/h) based on patient specific IV start and stop times to assist in modeling. To further assist in modeling, primary criteria parameters from NCA were used as initial estimates. Sequential time points and corresponding concentrations through the entire dosing regimen of 168 h were added to assist the modeling program. Although AUC was not a PK parameter originally derived from compartmental analysis, it was calculated based off the patient-specific absolute dose of LMP744 and CL_t values obtained. The following equation was used to determine each patient's AUC from compartmental data:

$$AUC = \frac{Dose}{Clearance}$$

Equation 3. Equation for AUC

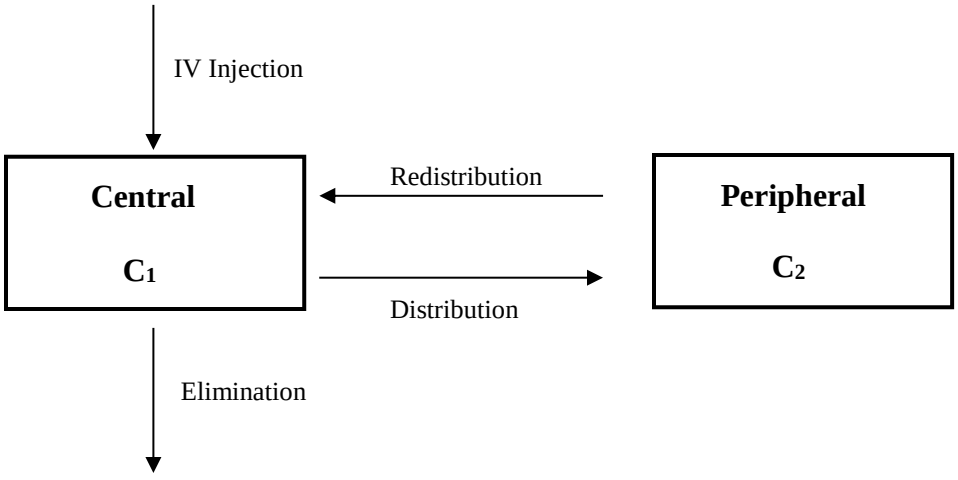

Figure 6. A simplified 2-compartment model showing drug absorbed into the first compartment via IV injection, with distribution and redistribution to and from a peripheral compartment followed by elimination of the drug from the central compartment

2.5.3 Comparison of NCA and Compartmental Modeling

Comparisons of NCA and compartmental modeling were performed by contrasting values calculated by each method. To do this, the PK parameter value calculated via NCA analysis was subtracted from the same parameter calculated from compartmental analysis. This value was then divided by the compartmental analysis value and represented as a percentage. The formula used for this method can be seen in **Equation 4**. Therefore, a percentage close to zero would represent little variation between the PK parameters generated from noncompartmental and compartmental modeling. The PK parameters that were analyzed are clearance, volume of distribution and half-life. Median, mean, standard deviation (SD), minimum (min) and maximum (max) comparison values were recorded. Interpatient variation was calculated by dividing the standard deviation by the mean and is expressed as a percentage (i.e. the coefficient of variation [CV%]).

$$\frac{(NCA - Compartmental)}{Compartmental} * 100$$

Equation 4. Equation for comparing PK parameters calculated from NCA and compartmental modeling

2.6 DOSE LINEARITY

Dose linearity of LMP744 was evaluated visually as well as according to Hummell *et al* on the basis that a drug and its correlating PK paramaters exhibit linearity if there is a value of "β = 1" from **Equation 2**. Dose linearity was assessed visually by observing plots of dose-normalized C_{max} vs absolute dose and dose-normalized AUC vs absolute dose of LMP744. To formally evaluate dose linearity, each patient's AUC and C_{max} values, were log-normalized and plotted vs

the log-normalized absolute dosage of administered LMP744. Dose linearity statistical analyses were conducted using GraphPad Prism 8 (San Diego, CA).

2.7 BSA AND WEIGHT AS COVARIATES

2.7.1 BSA as a Covariate on Clearance

To aid in the determination to suggest if a BSA-based dosing regimen should be recommended for the IV administration of LMP744, the effect that BSA had on clearance was analyzed. First, each patient's clearance values, calculated via noncompartmental modeling, were normalized to the mean clearance value for all 17 patients which resulted in mean-normalized clearance values (i.e. $Cl/Cl_{mean)}$. Additionally, patient-specific clearance values were first normalized to their BSA, then subsequently normalized to the mean clearance values for that specific parameter. Median, mean, standard deviation (SD), and the coefficient of variation (CV%) were included in all analyses. To test the homogeneity of variance between the two groups, an F-test was performed. A significant value of less than "0.05" was determined to suggest statistical significance. Statistical analyses were done using IBM SPSS Statistics (Armonk, New York).

2.7.2 Weight as a Covariate on Distribution Volume

To aid in the determination of whether volume of distribution is significantly affected by the patient's size, weight was used as a covariate. First, patient volume of distribution values were normalized to the mean V_c value for all 17 patients which resulted in mean-normalized V_c values

(i.e. V_c/V_{cmean}). Next, patient-specific V_c values were first normalized to their respective weights and subsequently normalized to the mean V_c values for that specific parameter (i.e. [V_c/Weight]/ [V_c/$Weight_{mean}$]).]). This process was repeated for both V_p and V_{ss} PK parameters. Median, mean, standard deviation (SD), and the coefficient of variation (CV%) were included in all analyses. To test the homogeneity of variance between the two groups, an F-test was performed. A significant value of less than "0.05" was determined to suggest statistical significance. Statistical analyses were done using IBM SPSS Statistics (Armonk, New York).

3.0 RESULTS

3.1 QUANTITATIVE LC-MS/MS ASSAYS

3.1.1 Assay Comparison

Plasma samples from patients treated at the lower LMP744 doses often contained LMP744 concentrations below the LLOQ of the FDA guidance validated assay. Therefore, in addition to the validated LC-MS/MS approach, a more sensitive novel assay was needed for the quantitative analysis of drug concentrations in human plasma. The regression for the validated LC-MS/MS assay was weighted $1/y^2$ and fit linearly ($y = 0.0253x - 0.7695$) with an R^2 coefficient of 0.999 (**Figure 7**). A triplicate standard curve prepared prior to sample analysis revealed the LMP744 assay to be accurate (93.1-103.8%) and precise (CV < 6.6%), see **Table 2**. The ratio of analyte area to internal standard area was used to back calculate the concentration based off the generated standard curve.

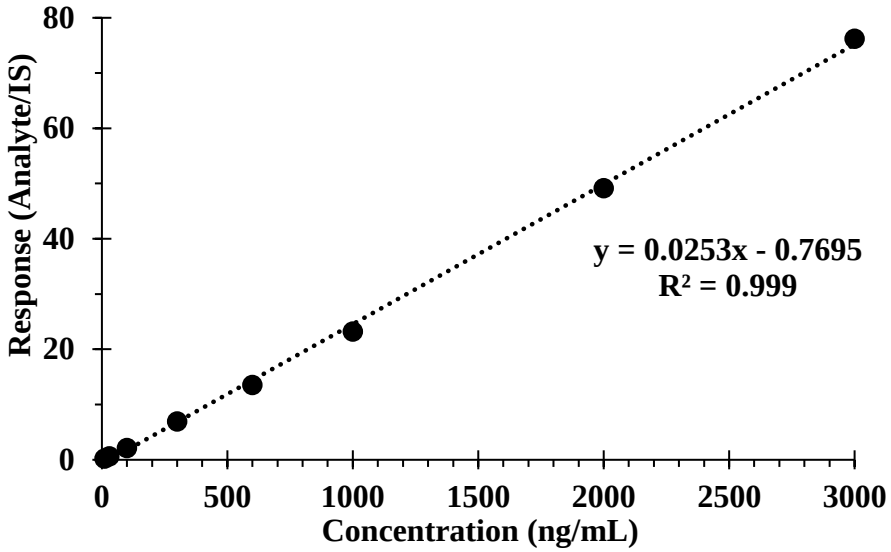

Figure 7. Average concentration values from a triplicate standard curve of LMP744 quantified using the validated LC-MS/MS assay, showing linearity over a concentration range of 10-3000 ng/mL with an R^2 value of 0.999.

Table 2. Assay performance data of the calibration samples of LMP744 in human plasma using the validated assay. Standard calibrators were run in triplicate and average concentration values were taken. QCs were run in duplicate and average concentration values were used.

	Conc. (ng/mL)	Bias (%)	Precision (%)
Calibrators*	10	2.1	1.4
	30	-3.8	4.7
	100	-1.5	3.0
	300	1.4	1.3
	600	-2.9	3.7
	1000	-1.3	4.7
	2000	3.2	5.4
	3000	6.9	4.8
QCs**	25	-9.9	5.8
	200	-3.8	0.1
	2500	-6.8	2.6

*n=3. **n=2

Quality control samples were run in duplicate prior to sample analysis. Results from **Table 2** suggest that QCs at all three levels were calculated accurately (100 – 109.9%) and precisely (CV < 5.8%).

The regression for the novel, more sensitive, assay was weighted $1/y^2$ and fit linearly ($y = 0.0063x - 0.0049$) with an R^2 coefficient of 0.999 (**Figure 8**). A triplicate standard curve prepared prior to sample analysis revealed the LMP744 assay to be accurate (90.6 - 112%) and precise (CV < 6.6%), see **Table 3**. The ratio of analyte area to internal standard area was used to back calculate the concentration based off the generated standard curve.

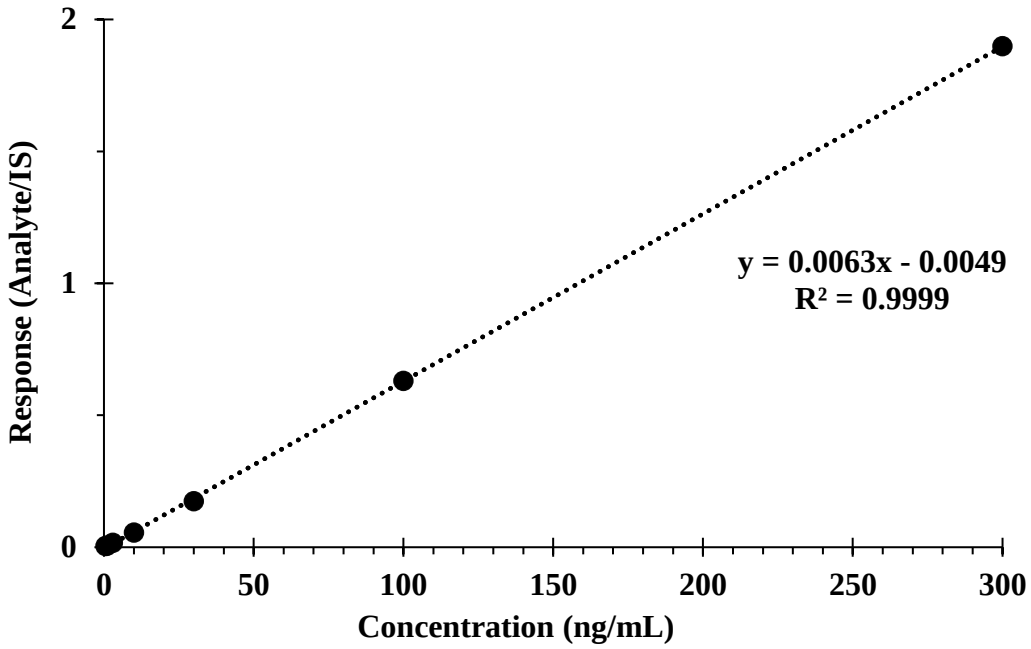

Figure 8. Average concentration values from a triplicate standard curve of LMP744 quantified using the novel, more sensitive, assay, showing linearity over a concentration range of 1-300 ng/mL with an R^2 value of 0.999

Table 3. Assay performance data of the calibration samples of LMP744 in human plasma using the, more sensitive, assay. Standard calibrators were run in triplicate and average concentration values were taken. QCs were run in duplicate and average concentration values were used.

	Conc. (ng/mL)	Bias (%)	Precision (%)
Calibrators*	1	-5.5	5.3
	3	9.4	3.7
	10	-4.5	3.3
	30	4.3	6.6
	100	-12.0	1.8
	300	-9.5	2.4
QCs**	2.5	12.3	9.0
	25	9.6	0.6
	200	-10	0.3

*n=3. **n=2

Quality control samples were run in duplicate prior to sample analysis. Results from **Table 3** suggest that QCs at all three levels were calculated accurately (87.7 – 110%) and precisely (CV < 9.0%).

3.1.2 Cross-Validation

To aid in the validation of the novel, more sensitive, assay, cross-validation studies with the validated LC-MS/MS proved that values generated were accurate. When comparing LMP744 concentration values generated from plasma samples that were originally within the validated limits of quantitation, values generated with the more sensitive assay were within acceptable range limits. The percent of deviation between individual drug concentrations is shown in **Figure 9**. Drug concentration was also assessed on a per-patient basis, which can be seen in **Figure 10**. Out

of 58 total samples cross-validated, 47 (81%) were shown to be within 20% of originally calculated concentrations.

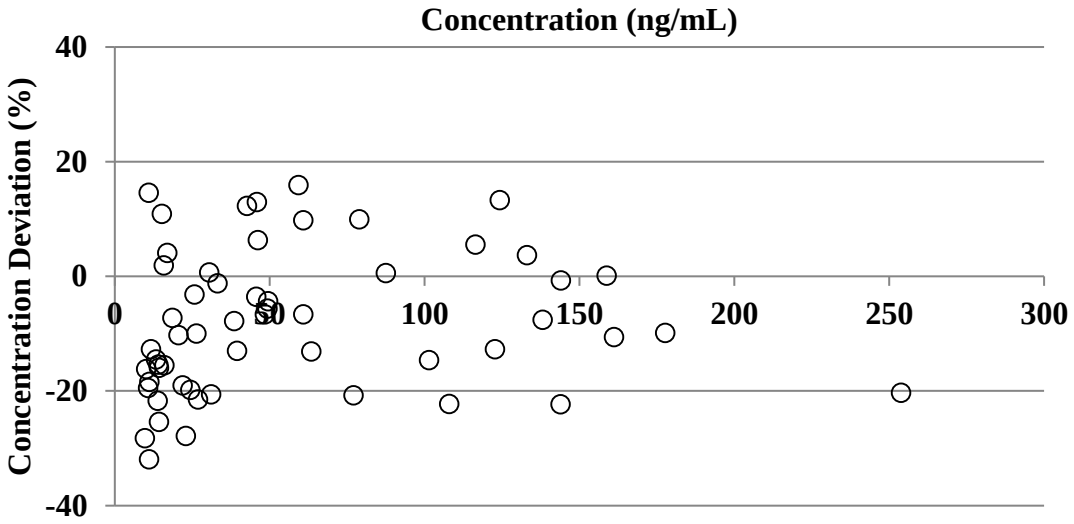

Figure 9. Concentrations deviations between drug concentrations originally calculated from the validated LC-MS/MS and the novel, more sensitive, assay, shown as percentages.

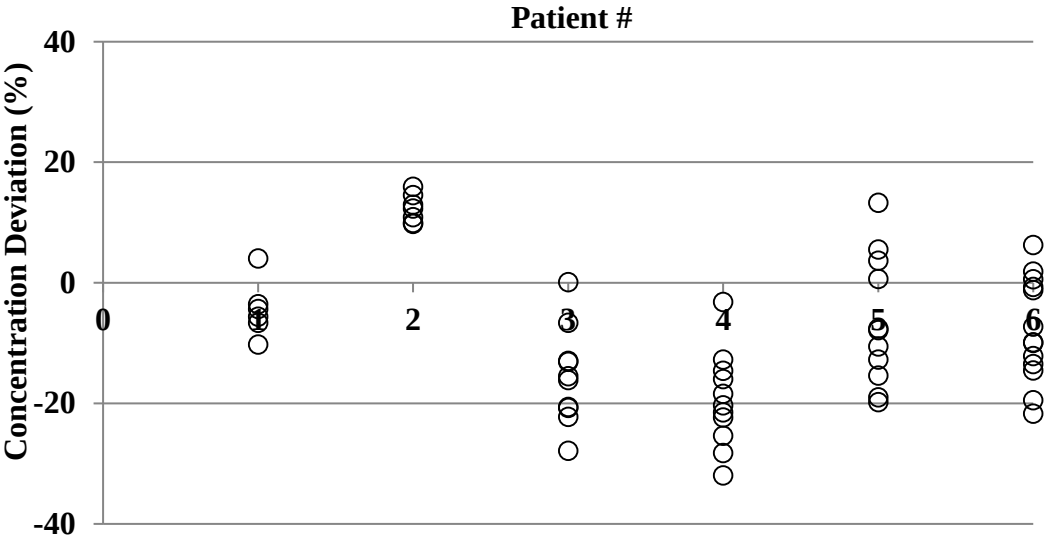

Figure 10. Deviations on a per-patient basis comparing drug concentrations originally calculated from the validated LC-MS/MS and the novel, more sensitive, assay, shown as percentages

3.2 PHARMACOKINETICS

Patients were dosed intravenously for 1 hour every 24 hours for a total of 5 days. Basic patient demographics are listed in **Table 4**. Plasma concentration-time profiles for all 17 patients dosed IV are listed below based on dose level of LMP744. In addition to plasma, urine from every patient was collected for 24 h post initial infusion of LMP744. The amount of the recovered dose of LMP744 excreted in urine, per patient can be found in **Figure 17**. Negligible concentrations, less than 5% of dose administered, were recovered per patient across the dosing range.

Table 4. Demographics of patients receiving a daily infusion of LMP744

Demographics	
Parameters	**Number of Patients**
Number of patients enrolled	17
Male/female	11/5*
Median age, years (range)	58.5 (42 - 84)*
Tumor type	
Colorectal cancer	2
Pancreatic cancer	1
Rectal cancer	1
Colon cancer	6
Adenocarcinoma	1
Hodgkin lymphoma	1
Head and neck cancer	1
Mesothelioma	1
Cholangiocarcinoma	1
Not Provided	2*

*Complete patient demographics unavailable

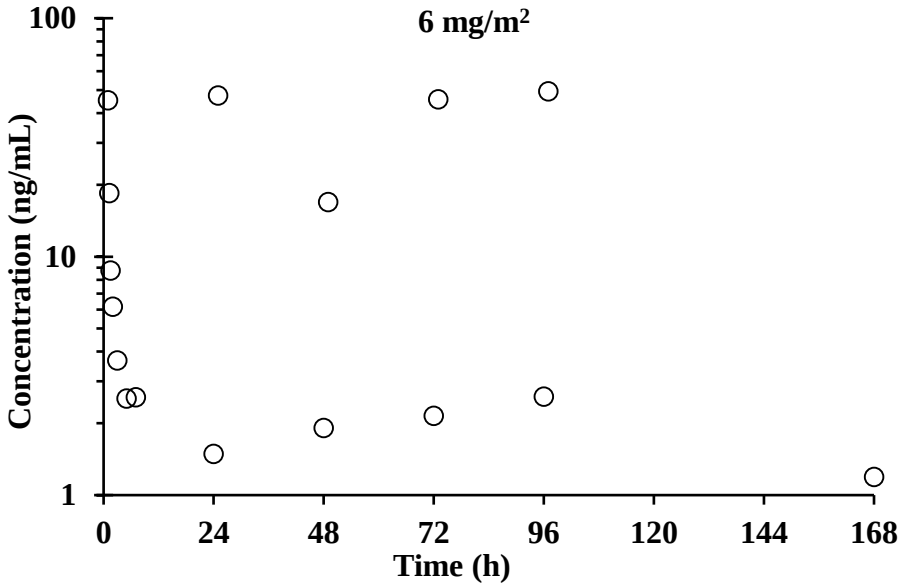

Figure 11. Concentration vs time results from 1 patient receiving daily 1 hour infusions of LMP744 for 5 days at the dosing level of 6 mg/m^2

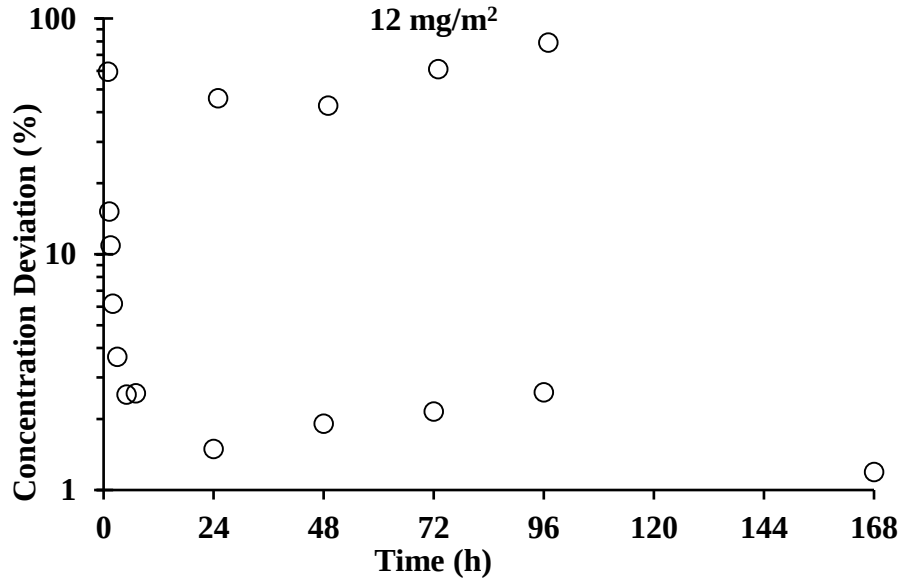

Figure 12. Concentration vs time results from 1 patient receiving daily 1 hour infusions of LMP744 for 5 days at the dosing level of 12 mg/m^2

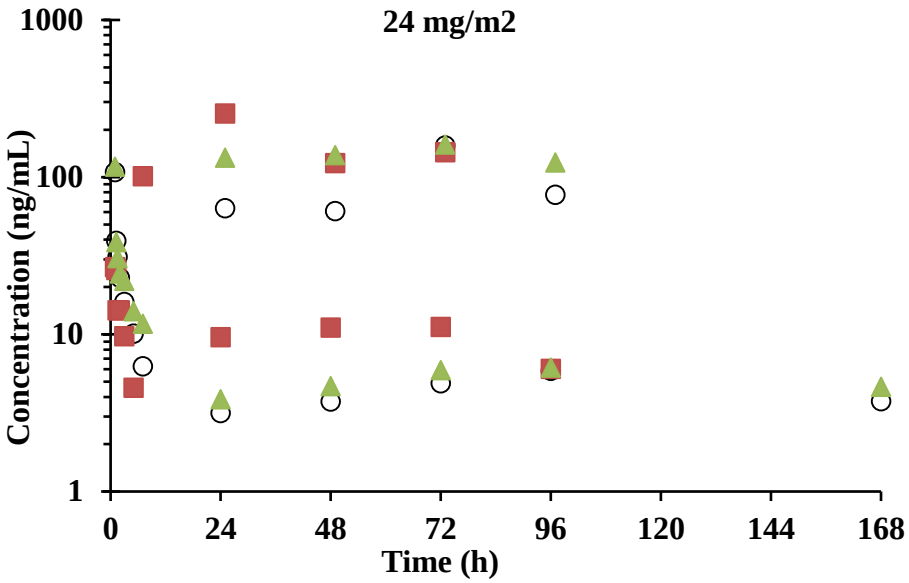

Figure 13. Concentration vs time results from 3 patients receiving daily 1 hour infusions of LMP744 for 5 days at the dosing level of 24 mg/m^2

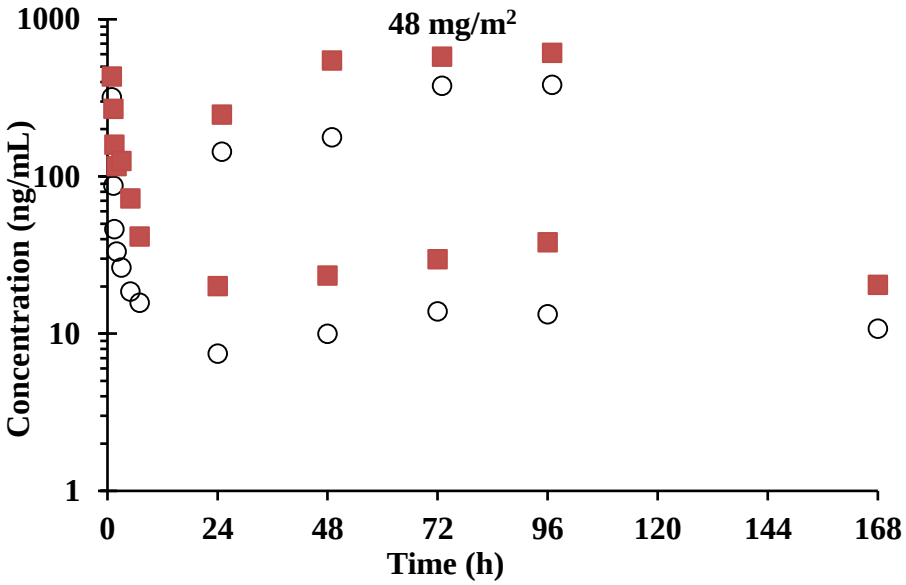

Figure 14. Concentration vs time results from 2 patients receiving daily 1 hour infusions of LMP744 for 5 days at the dosing level of 48 mg/m^2

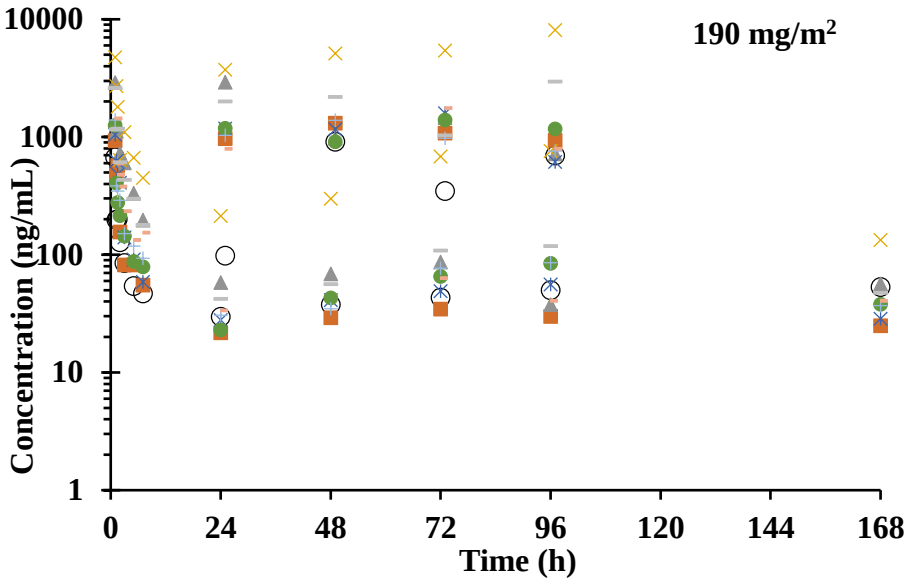

Figure 15. Concentration vs time results from 9 patients receiving daily 1 hour infusions of LMP744 for 5 days at the dosing level of 190 mg/m^2

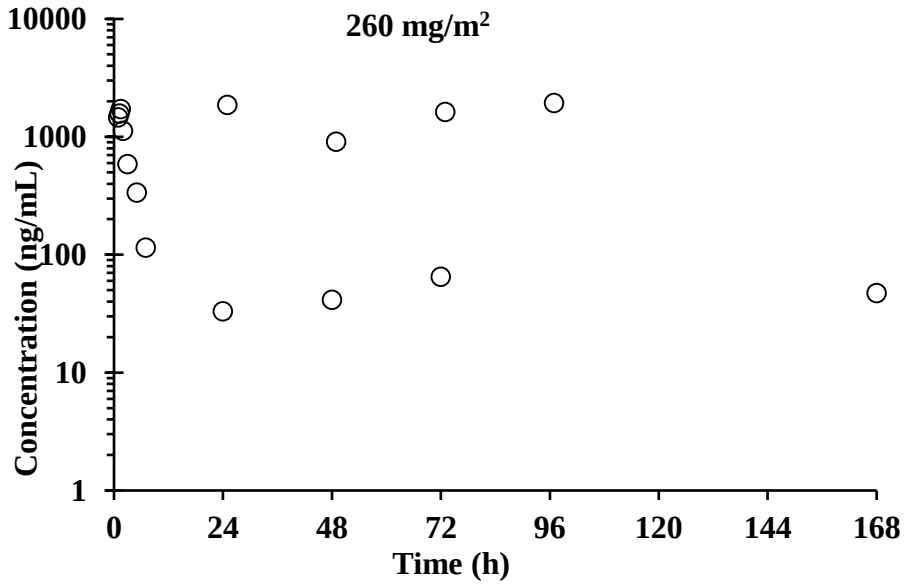

Figure 16. Concentration vs time results form 1 patient receiving daily 1 hour infusions of LMP744 for 5 days at the dosing level of 260 mg/m^2

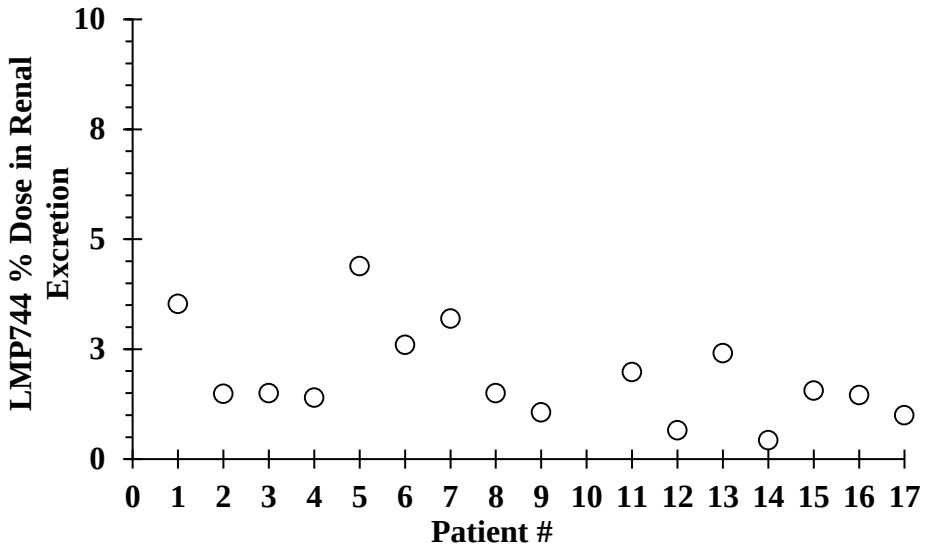

Figure 17. Amount of the LMP744 administered dose recovered in urine from each patient

3.2.1 Noncompartmental Modeling Analysis

Pharmacokinetic parameters were first calculated noncompartmentally through the first 24 h. To calculate the percentage of AUC extrapolation to infinite time, the following equation was used:

$$\%\, Extrapololated = \frac{(AUCinf - AUC)}{AUCinf} * 100$$

Equation 5. Equation for extrapolated AUC

A value of less than 20% would suggest appropriate AUC extrapolation to infinity. However, median and mean values were indeed greater than 20% (21.1 and 20.5%, respectively) with a high coefficient of variation (50.1%), which can be seen in **Table 5**. The remaining PK parameters (T_{max}, C_{max}, $t_{1/2}$, Cl, V_{ss} and V_d**)** for all 17 patients are listed in **Table 6**. Although the

C_{max} of LMP744 differed by patient and dose level, T_{max} remained consistent at 1 h. This is most likely due to sampling timing of 2 min prior to the end of the 1 h infusion.

Table 5. Noncompartmental AUC parameters of LMP744 in humans derived from the first 24 h

PT #	AUC_{0-24} µg/L * h	$AUC_{0-\infty}$ µg/L * h	% Extrapolated*
1	91.7	142	35.4
2	117	162	27.9
3	141	178	21.1
4	106	156	32.4
5	185	259	28.6
6	357	462	22.8
7	1388	1857	25.3
8	1577	2580	38.8
9	2034	2429	16.2
10	7046	7853	10.2
11	13924	18810	25.9
12	2493	2999	16.9
13	2496	2819	11.4
14	2930	3374	13.1
15	3893	4319	9.88
16	6147	6585	6.66
17	5781	6104	5.30
Median	2034	2581	21.1
Mean	2983	3594	20.5
S.D.	3610	4609	10.3
CV%	121	128	50.1

*Calculated using **equation 5**

Table 6. Remaining PK parameters of LMP744 in humans derived with NCA

PT #	T_{max} h	C_{max} ng/mL	$t_{1/2}$ h	Cl L/h	V_{ss} L	V_d L
1	1	48.4	23.4	100	2459	3394
2	1	69.6	19.1	144	2684	3987
3	1	86.3	14.4	180	2768	3734
4	1	24.9	3.63	174	3879	3982
5	1	116	4.41	189	1059	226
6	1	318	4.66	210	985	3339
7	1	433	16.2	72.4	1209	1826
8	1	670	23.3	184	4919	6305
9	1	930	12.6	212	2386	3401
10	1	2909	9.66	42.8	357	594
11	1	4760	15.8	22.1	323	411
12	1	1044	12.6	112	1559	2626
13	1	1257	9.72	158	1411	2222
14	1	1395	10.1	116	1135	1685
15	1	1438	8.77	91.1	781	1152
16	1	2614	7.21	55.5	371	577
17	1	1718	6.76	64.8	379	632
Median	1.0	931	21.1	116	1209	2222
Mean	1.0	1167	20.5	126	1680	2348
S.D.	0	1276	10.3	61.4	1327	1703
CV%	0	109	50.1	48.9	79.0	72.5

3.2.2 Compartmental Modeling

Compartmental modeling of LMP744 data showed that a 2-compartment model best fit the data set provided from plasma samples of all 17 patients. All PK parameters generated from compartmental modeling can be seen in **Table 7**. Since AUC was not a provided PK parameter from modeling and is dependent on total clearance and dose administered, **Equation 3** was utilized to calculate AUC across the entire dosing range.

Table 7. Plasma PK parameters and R^2 values derived from 2-compartmental modeling analysis of LMP744 in humans.

PT #	R^2	Cl_t L/h	Cl_d L/h	V_c L	V_p L	$t_{1/2}$ h	AUC* (µg/L * h)
1	0.991	94.8	232	119	2466	26.0	150
2	0.915	151	281	139	3307	23.7	155
3	0.743	136	277	355	3436	27.3	363
4	0.794	81.1	220	152	2473	29.9	642
5	0.933	98.7	273	274	2526	25.6	498
6	0.885	91.6	285	87.9	2878	29.3	1063
7	0.813	59.1	83.1	254	1826	38.4	2265
8	0.829	136	625	355	6247	40.2	3488
9	0.959	159	306	252	3891	26.5	3244
10	0.632	45.2	31.8	168	1026	36.9	7446
11	0.899	14.3	68.4	20.4	334	20.5	27466
12	0.851	93.4	122	230	2280	30.9	3864
13	0.914	103	252	217	2957	28.9	4301
14	0.870	85.2	239	218	2265	26.3	4614
15	0.796	66.4	209	220	1802	26.6	5927
16	0.834	45.1	33.2	150	992	36.9	8094
17	0.893	53.5	32.6	184	1535	53.5	5398
Median	0.87	91.6	232	217	2466	28.9	-
Mean	0.86	89.1	210	199	2484	31.1	-
S.D.	0.09	40.2	146	87.4	1345	7.98	-
CV%	10.09	45.1	69.6	43.8	54.2	25.7	-

* Calculated using **equation 3**

3.2.3 Comparison of NCA and Compartmental Modeling

The PK parameters chosen for comparison were clearance, volume of distribution and half-life. All comparisons are from values originally generated from NCA and compartmental modeling analyses. **Equation 4** was used to calculate absolute values, displayed as percentages, shown in **Table 8**.

Table 8. Comparison of clearance, volume of distribution and half-life values derived by NCA relative to compartmental modeling.

PT #	ΔCl (%) L/h	Abs. ΔCl (%) L/h	ΔV_d (%) L	Abs. ΔV_d (%) L	$\Delta t_{1/2}$ (%) h	Abs. $\Delta t_{1/2}$ (%) h
1	6.11	6.11	-4.56	4.56	-10.1	10.1
2	-4.36	4.36	-23.1	23.1	-19.5	19.5
3	32.3	32.2	-30.5	30.5	-47.4	47.4
4	116	116	13.9	13.9	-87.9	87.9
5	91.7	91.7	-93.8	93.8	-82.8	82.8
6	129	129	-13.7	13.7	-84.1	84.1
7	22.4	22.4	-44.3	44.3	-57.8	57.8
8	35.2	35.2	-20.3	20.3	-41.8	41.8
9	33.5	33.5	-44.1	44.1	-52.3	52.3
10	-5.15	5.15	-75.3	75.3	-73.9	73.9
11	55.1	55.1	-2.27	2.27	-22.6	22.6
12	20.2	20.2	-36.9	36.9	-59.2	59.2
13	52.6	52.6	-48.7	48.7	-66.4	66.4
14	36.5	36.5	-47.9	47.9	-61.8	61.8
15	37.3	37.3	-54.7	54.7	-67.1	67.1
16	23.1	23.1	-76.0	76.0	-80.5	80.5
17	-11.6	11.6	-88.8	88.8	-87.4.36	87.4
Median	33.5	33.5	-44.0	44.0	-61.8	61.8
Mean	39.4	41.9	-40.6	42.3	-59.0	59.0
S.D.	40.2	37.4	30.9	28.5	24.2	24.2
CV%	101	89.2	-76.0	67.3	-41.1	41.1
Min	-11.6	4.36	-93.8	2.27	-87.9	10.1
Max	129	130	13.9	93.8	-10.1	87.9

3.3 DOSE LINEARITY OF LMP744

Dose linearity was assessed visually and formally based on PK parameters C_{max} and AUC. To assess visual linearity, C_{max} and AUC were both normalized to their corresponding doses, see **Table 9**. These PK parameters were then individually plotted vs the absolute dose, see **Figure 18** and **Figure 19**. Visually, dose linearity based on C_{max} and AUC appears to be evident. Formally evaluating dose linearity required the use of log-normalized values of C_{max} and AUC, along with log-normalized dosages. Log-normalized values can be seen in **Table 10.** When plotting vs the natural log of the dose, corresponding log-normal C_{max} and AUC relationships become linear. These relationships can be seen in **Figure 20** and **Figure 21**, respectively.

3.3.1 Dose Normalization

Visual linearity between C_{max} and AUC, when normalized to dose can be observed in **Figure 18** and **Figure 19**. The slight C_{max} and AUC variability shown, resulting in a high concentration, can mostly likely be due to sampling timing error. A sample drawn closer to the end of infusion, or with a higher infusion rate, of LMP744 could explain the higher concentrations seen in these figures. Dose normalized values of these PK parameters are shown in **Table 9**.

Table 9. Dose normalized C_{max} and AUC values of LMP744 administered in humans

PT #	C_{max}/Dose ng/mL/mg	AUC/Dose (ng/mL*h)/mg
1	3.39	9.94
2	2.96	6.90
3	1.75	5.55
4	0.48	5.72
5	2.37	5.28
6	3.27	4.75
7	3.23	13.8
8	1.41	5.42
9	1.80	4.71
10	8.65	23.4
11	12.2	45.2
12	2.89	8.91
13	2.82	6.31
14	3.55	8.60
15	3.66	10.9
16	7.17	18.1
17	4.35	15.4
Mean	3.88	11.7
Median	3.23	8.60
S.D.	2.91	10.1

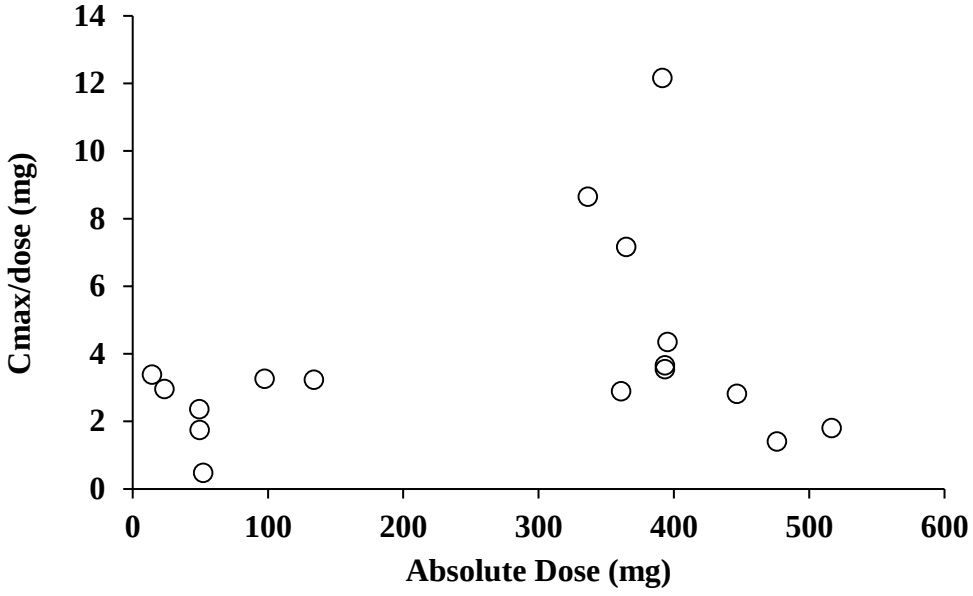

Figure 18. Dose normalized C_{max} concentrations vs absolute dose of administered LMP744

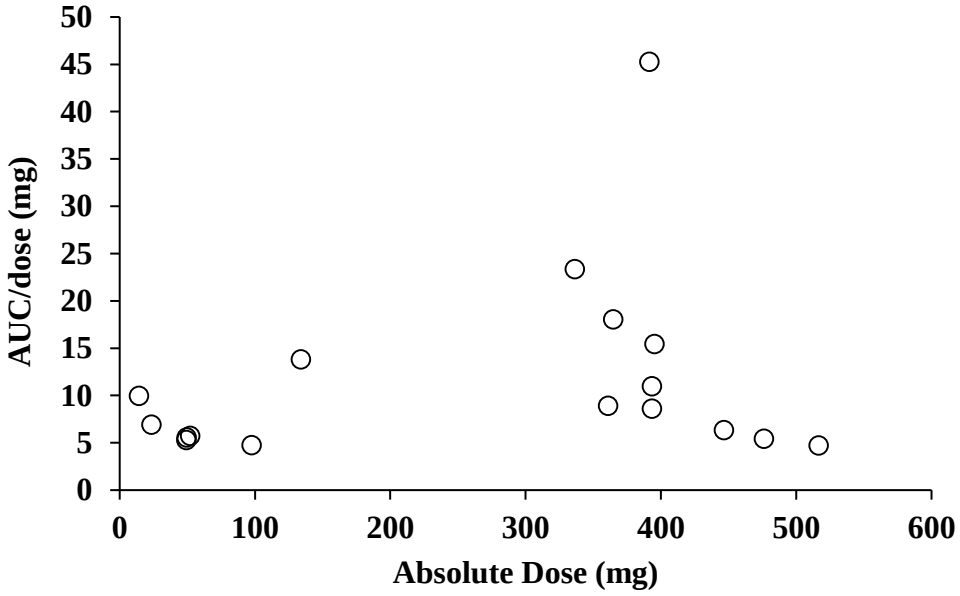

Figure 19. Dose normalized AUC values vs absolute dose of administered LMP744

3.3.2 Log-Normal Transformation

Log-normal transformation of dose, C_{max}, and AUC was performed to properly assess dose linearity across the entire dose of all patients receiving intravenous LMP744. Following a log-normal transformation, C_{max} vs absolute dose showed a linear relationship. Log-normal C_{max} vs log-normal dose provided a line of best fit with an R^2 value of 0.809 (**Figure 20**). When introduced into the linear power model (**Equation 2**) the slope, β, had a caluculated value of 1.20 (0.94 – 1.47: 90% CI). In a addition, following log-normal transformation, AUC vs absolute dose, also showed a linear relationship. A line of best fit provided an R^2 value of 0.860 (**Figure 21**). When this was introduced into the same linear power model the slope, β, had a calculated value of 1.17 (0.95 - 1.38: 90% CI).

Table 10. Log-normalized absolute dosages, C_{max} and AUC values of LMP744 in humans

PT #	LN Dose mg	LN C_{max} mL	LN AUC mg/L*h
1	2.66	3.88	-1.89
2	3.16	4.24	-1.86
3	3.90	4.46	-1.01
4	3.95	3.21	-0.44
5	3.90	4.76	-0.70
6	4.58	5.76	-0.06
7	4.90	6.07	0.82
8	6.17	6.51	1.25
9	6.25	6.84	1.18
10	5.82	7.98	2.01
11	5.97	8.47	3.31
12	5.89	6.95	1.35
13	6.10	7.14	1.46
14	5.97	7.24	1.53
15	5.97	7.27	1.78
16	5.90	7.87	2.09
17	5.98	7.45	2.00
Mean	5.12	6.24	0.76
Median	5.89	6.84	1.25
S.D.	1.19	1.59	1.49
CV%	23.2	25.4	196

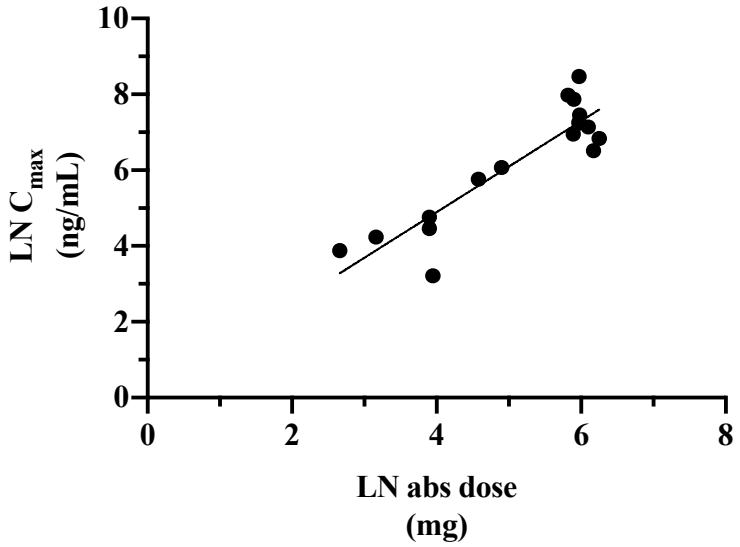

Figure 20. Log-normal C_{max} vs log-normal absolute dose of LMP744

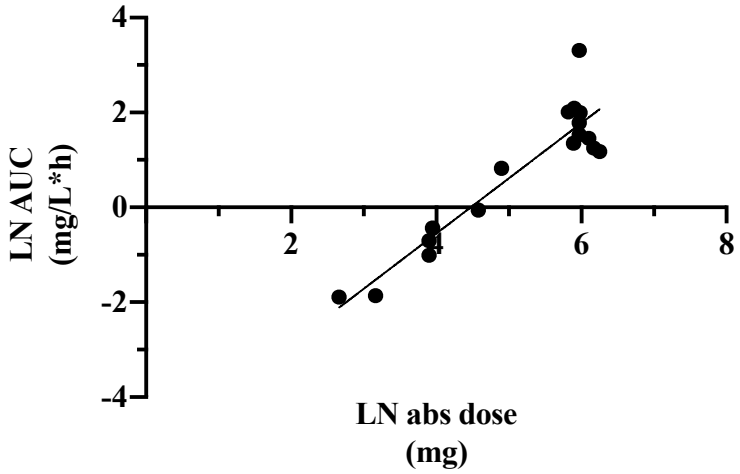

Figure 21. Log-normal AUC vs log-normal absolute dose of LMP744

3.4 BSA AND WEIGHT AS COVARIATES

BSA-normalized clearance and weight-normalized $V_{c,}$ V_p, and V_{ss} values for each patient, can be seen below in **Table 11.** For BSA-normalized clearance; mean, median and standard deviation values were 42.8, 42.3 and 16.6, respectively. For weight weight-normalized $V_{c;}$ mean, median and standard deviation values were 2.3, 2.2, and 1.3, respectively. For weight weight-normalized $V_{p;}$ mean, median and standard deviation values were 26.3, 25.4, and 43.7, respectively. For weight weight-normalized $V_{ss;}$ mean, median and standard deviation values were 17.3, 11.3, and 12.2, respectively.

Table 11. BSA-normalized clearance and weight-normalized volume of distribution values for patients administered LMP744 as derived with compartmental modeling.

PT #	Cl/BSA L/h/m^2	V_c/Weight L/kg	V_p/Weight L/kg	V_{ss}/Weight L/kg
1	39.8	1.04	21.7	21.6
2	77.3	1.44	34.3	27.9
3	66.1	4.06	39.4	31.7
4	37.4	1.56	25.4	39.9
5	48.2	2.61	24.1	10.1
6	45.1	1.01	33.1	11.3
7	42.3	5.39	38.8	25.7
8	55.0	2.85	50.2	39.5
9	59.2	1.87	28.9	17.7
10	25.5	2.44	14.9	5.18
11	6.92	0.22	3.58	3.46
12	49.2	3.26	32.3	22.1
13	44.2	1.19	16.2	7.75
14	41.2	2.18	22.6	11.3
15	32.1	2.44	20.0	8.67
16	23.5	1.72	11.4	4.25
17	35.2	3.65	30.5	5.50
Mean	42.8	2.3	26.3	17.3
Median	42.3	2.2	25.4	11.3
S.D.	16.6	1.3	43.7	12.2

3.4.1 BSA as a Covariate on Clearance

To properly evaluate if BSA held a role in the clearance of LMP744, all patient clearance levels were first normalized to their mean. Additionally, BSA-normalized clearance values were also normalized to their specific mean, results are shown in **Table 12**. Mean-normalized clearance values provided a median, mean, standard deviation and coefficient of variation of 1.0, 1.0, 0.45 and 45.1%, respectively. Whereas, patient clearance originally normalized to patient BSA and then

normalized to its mean, resulted in a median, mean, standard deviation and coefficient of variation of 1.0, 1.0, 0.40 and 38.7%, respectively.

Table 12. Total clearance of LMP744 normalized by the average patient clearance from compartmental analysis and BSA normalized clearance values normalized by its mean.

PT #	Cl / Cl_{mean}	CL/BSA / Cl_{mean}
1	1.07	0.94
2	1.72	1.83
3	1.54	1.56
4	0.92	0.88
5	1.12	1.14
6	1.04	1.07
7	0.67	1.00
8	1.55	1.30
9	1.80	1.40
10	0.51	0.60
11	0.16	0.16
12	1.06	1.16
13	1.18	1.05
14	0.97	0.97
15	0.75	0.76
16	0.51	0.56
17	0.60	0.80
Median	1.0	1.0
Mean	1.0	1.0
S.D.	0.45	0.40
CV%	45.1	38.7

An F-Test was used to determine if the CV% of the BSA-normalized clearance was significantly lower than the CV% of the absolute clearance. Even though the coefficient of variation reduced from 45.1% to 38.7%, a P-value of 0.477 ultimately suggested that variance in clearance between the two groups were not statistically different from one another. The results from the F-test that was performed to test the homogeneity of variances can be found in **Table 13**.

Table 13. Statistical results from F-test showing a lack of significant difference between variances of LMP744 clearance and BSA-normalized LMP744 clearance in humans.

Test of Homogeneity of Variances				
	Levene Statistic	df_1	df_2	Sig.
Clearance	0.517	1	32	0.477

*No statistical significance

3.4.2 Weight as a Covariate on Distribution Volume

To properly evaluate if weight played a significant role in the volume of distribution of LMP744, all patient V_c, V_p, and V_{ss} levels were first normalized to their mean. Weight-normalized values were also normalized to their specific mean and results are shown in **Table 14**. Mean-normalized V_c values provided a median, mean, standard deviation and coefficient of variation of 1.0, 1.0, 0.44 and 43.8%, respectively. Whereas, patient V_c originally normalized to patient weight and then normalized to the mean, resulted in a median, mean, standard deviation and coefficient of variation of 1.0, 1.0, 0.60 and 56.1%, respectively. Mean-normalized V_p values provided a median, mean, standard deviation and coefficient of variation of 1.0, 1.0, 0.54 and 54.2%, respectively. Patient V_c originally normalized to patient weight and then normalized to the mean, resulted in a median, mean, standard deviation and coefficient of variation of 1.0, 1.0, 0.40 and 43.7%, respectively. Lastly, mean-normalized V_{ss} values provided a median, mean, standard deviation and coefficient of variation of 0.7, 1.0, 0.80 and 79.0%, respectively. Patient V_{ss} originally normalized to patient weight and then normalized to the mean, resulted in a median, mean, standard deviation and coefficient of variation of 0.7, 1.0, 0.70 and 70.5%, respectively

Table 14. Volume of distribution of LMP744 normalized by the average volume of distribution and volume of distribution normalized by patient weight normalized by the average.

PT #	V_c/ V_{cmean}	V_c/Weight/ V_{cmean}	V_p/ V_{pmean}	V_p/Weight/ V_{pmean}	V_{ss}/ V_{ssmean}	V_{ss}/Weight/ V_{ssmean}
1	0.59	0.46	1.00	0.82	1.46	1.25
2	0.70	0.63	1.34	1.31	1.60	1.61
3	1.78	1.78	1.40	1.50	1.65	1.84
4	0.76	0.68	1.01	0.97	2.31	2.31
5	1.37	1.14	1.03	0.91	0.63	0.59
6	0.44	0.44	1.17	1.26	0.59	0.66
7	1.27	2.35	0.74	1.47	0.72	1.49
8	1.78	1.25	2.54	1.91	2.93	2.29
9	1.26	0.82	1.58	1.10	1.42	1.03
10	0.84	1.06	0.42	0.57	0.21	0.30
11	0.10	0.10	0.14	0.14	0.19	0.20
12	1.15	1.42	0.93	1.23	0.93	1.28
13	1.09	0.52	1.20	0.62	0.84	0.45
14	1.09	0.95	0.92	0.86	0.68	0.66
15	1.10	1.07	0.73	0.76	0.47	0.50
16	0.75	0.75	0.40	0.43	0.22	0.25
17	0.92	1.59	0.62	1.16	0.16	0.32
Median	1.0	1.0	1.0	1.0	0.7	0.7
Mean	1.0	1.0	1.0	1.0	1.0	1.0
S.D.	0.44	0.60	0.54	0.40	0.80	0.70
CV%	43.8	56.1	54.2	43.7	79.0	70.5

An F-Test was used to determine if the CV% of the weight-normalized V_c was significantly lower than the CV% of the absolute V_c. Even though the coefficient of variation increased from 43.8% to 56.1%, a P-value of 0.400 ultimately suggested that variance in V_c between the two groups were not statistically different from one another. The coefficient of variation decreased in both peripheral and steady state volume of distribution groups, however neither were found to be statistically significant changes from their respective cohort. The results from the F-test that was performed to test the homogeneity of variances can be found in **Table 15**.

Table 15. Statistical results from F-test showing a lack of statistical significance between weight and volume of distribution of LMP744 in humans.

Test of Homogeneity of Variances				
	Levene Statistic	df_1	df_2	Sig.
Central Volume of Distribution	0.728	1	32	0.400
Peripheral Volume of Distribution	0.074	1	32	0.788*
Steady State Volume of Distribution	0.058	1	32	0.811*

*No statistical significance

4.0 DISCUSSION

To date, there is only one class of TOP1 inhibitors, camptothecins, that is FDA approved for the use in humans with various cancers. However, due to limitations such as chemical instability, short half-lives and severe side effects, there is a need for non-camptothecin TOP1 inhibitors. LMP744 is a novel, non-camptothecin, indenoisoquinoline derivative and TOP1 inhibitor with anticancer activity.

When compared to CPT derivatives, LMP744 has been shown to induce more stable TOP1cc which could lead to a more advantageous cancer therapy due to shorter drug infusions[28]. In addition, no metabolic activation is needed for therapeutic benefit of LMP744, unlike the CPT-derivative, irinotecan which must be bioactivated via hydrolysis to its active metabolite. LMP744 has also been shown to have a faster TOPcc rate constant than for CPT derivatives, which may lead to enhanced and strengthened TOPcc formation in cancer patients. While LMP744 has been shown to induce TOPcc while in the presence of CPT-resistant TOP1 enzymes, it is not a DNA intercalator and has shown no evidence of unwinding DNA in the absence of TOP1 [18]. TOPcc induced by LMP744 have been shown to be more persistent upon drug removal than those induced by CPT derivatives. Ultimately, LMP744 has been shown to inhibit TOP1 mediated DNA relaxation. This, along with the present data, may give rise to a more patient-friendly dosing regimen in cancer patients receiving intravenous doses of LMP744. A daily infusion may not be needed, and perhaps a weekly infusion is sufficient for durable target engagement.

The goal of this study was to quantitate plasma concentrations of LMP744 in humans receiving IV doses of LMP744 and utilize noncompartmental and compartmental modeling software to generate pharmacokinetic parameters. These PK parameters were then used to identify

dose linearity and evaluate the effect of patient BSA on LMP744 clearance and the effect of body weight on volume of distribution. A variety of methods were used in this study, including the implementation of a novel, more sensitive, assay which helped identify plasma drug concentrations at levels of quantitation that were previously below the limit of quantitation derived from our validated LC-MS/MS assay. These low concentrations are mostly likely due to the low absolute dose of LMP744 administered to these patients. In addition to analysis of samples that were below the original LLOQ, patient samples that were previously within detection limits were also re-run using our more sensitive assay to cross-validate the method. This method was cross-validated with our validated LC-MS/MS assay. Out of 58 total plasma samples that were re-analyzed with the more sensitive method, 47 (81%) proved to be within the acceptable concentration deviation of 20%. According to FDA guidance, acceptance criteria for ISR should have at least 67% of total samples be within ± 20% which means our 2 assays were successfully cross-validated [30].

Noncompartmental analysis is a method that characterizes pharmacokinetics of a drug. without assuming a specific number of compartments, allowing for a quick and simple method for evaluating drug exposure. To estimate the area under the plasma drug concentration-time curve, NCA utilizes the trapezoidal rule. However, the degree of error that is associated with this estimation depends on how well the width of each trapezoid fits in relation to the curvature of the true concentration-time profile. Consequently, using this trapezoidal rule will over-estimate the area during the elimination phase, while underestimating the area during the absorption or infusion phase. Therefore, calculating $AUC_{0\text{-}24}$ is not an accurate representative value of systemic exposure using the linear trapezoidal rule. The underestimation of systemic exposure is also seen in the percentage of AUC extrapolated to infinity from 24 h. Ideally, limits of extrapolation should be less than 20% and mean, standard deviation and coefficient of variation values of 20.5, 10.3 and

50.1%, respectively, proved that NCA was underestimating true AUC values. NCA also provided half-life values that indicate steady state pharmacokinetics beyond the sampling period of 24 h. Steady state pharmacokinetics are reached in four to five half-lives if given at a regular interval [31]. To properly evaluate exposure PK parameters such as AUC and Cl, steady must be reached, since both rely on an accurate representation of the true terminal half-life. Since our NCA of LMP744 only included the first 24 h of sampling, this was found to not be an accurate analysis of LMP744 pharmacokinetics. To address this issue, compartmental modeling was performed, incorporating 5 days worth of PK data, to ensure steady state was reached . LMP744 was best fit to a 2-compartmental model, assuming instantaneous drug distribution into the central compartment followed by slower distribution and redistribution to and from the peripheral compartment. No significant accumulation of LMP744 can mostly likely be attributed to the biphasic profile of LMP744 following IV bolus infusion for 5 consecutive days. Based on LMP744 terminal half-life, the terminal phase of the PK profile is expected to accumulate to some degree. However, this would only impact the terminal phase of the PK profile. Since the terminal phase has considerably less concentration of LMP744, this is not a major contributor to AUC. Thus, offering some explanation as to why no significant increase in systemic exposure of LMP744 is seen over time.

Liver metabolism is the major route of elimination for a wide variety of drugs and it can be affected by various parameters. Hepatic drug clearance may be defined as the total volume of blood that is able to perfuse through the liver which is then cleared from the body per unit time [32]. Three major parameters help facilitate hepatic metabolism and elimination, these include: blood flow through the liver, the free fraction of drug in the blood which is not bound to plasms proteins ultimately capable of interacting with hepatic enzymes, and the overall intrinsic ability of

the liver enzymes to metabolize the drug (i.e. intrinsic clearance). On average, the total hepatic blood flow in normal adults is approximately 1500 mL/min or 90 L/h. The ratio of the hepatic clearance to the hepatic blood flow is called the extraction ratio [32]. The extraction ratio of a drug can be used to assist in the classification of a high or low clearance drug, according to the amount of drug cleared through the liver. Drugs with a high extraction ratio (> 0.7), or high clearance drugs, are cleared from the blood by the liver at a rapid rate. Increasing blood flow to the liver would ultimately cause increased drug clearance and vice versa. Therefore, drugs with high hepatic clearance depend primarily on hepatic blood flow. Alternatively, drugs which have a low calculated extraction ratio, are not efficiently cleared by the liver and are cleared less extensively from the blood. Drugs with low hepatic clearance depend primarily on the intrinsic activity of metabolizing liver enzymes and by the free fraction of the drug. Consequently, clearance of these drugs is relatively independent from hepatic blood flow. On average, LMP744 was found to be a high clearance drug with an extraction ratio of approximately 0.94, significantly cleared from the liver with negligible renal clearance. We can also conclude that, due to the negligible renal clearance, the clearance of LMP744 is mostly hepatic, and likely metabolic. Therefore, changes in intrinsic hepatic clearance or free fraction of LMP744 would not significantly alter the total clearance of the drug.

A critical component in the drug development process is to recognize if dose linearity exists in humans. This helps to facilitate dosing regimens while maximizing therapeutic benefit. Dose escalation studies provide a way in which to analyze PK parameters and identify dose linearity across a large dose range. Based on the presented evidence, dose-linearity of LMP744 was found across the entire dose range of 6 to 190 mg/m^2, with proportional increases in exposure parameters C_{max} and AUC. This is suggested from not only visually evaluating dose-normalized PK

parameters, C_{max} and AUC, but also formally analyzing them, by use of the power model. Current FDA guidelines suggest that confidence intervals for the slope of linearity used for dose proportionality studies be set at (0.8, 1.25) [22]. While the slope of log-normal C_{max} vs log-normalized dose is 1.210 (0.94 – 1.48: 90% CI) the upper end of this confidence interval is outside the acceptable range. A similar trend is seen with log-normalized AUC vs log-normalized dose in that the slope generated from the line of best fit is 1.171 (0.95 – 1.39: 90% CI). The upper end of this confidence interval also falls outside the acceptable range set by the FDA, suggesting that linearity cannot be declared. However, a study from Hummel *et al* finds that these parameters are too strict and when assessing dose linearity across a complete dose range (i.e. dose escalation studies), more lenient criterion should be utilized with 90% confidence intervals [24]. Therefore, acceptable lower limit value will change to "ϑ_L = 0.5" and upper value to "ϑ_H = 2.0", as recommended. Ultimately, with these parameters, formal dose linearty can now be concluded, based on suggestions from Hummel *et al* [24] and observational analysis.

BSA-based dosing has been widely adopted as a standard practice for administration of several IV cytotoxic agents in the hopes that individualized patient adminsitraiton will reduce variability in exposure and optimize clinical benefit. Unfortunately, with many anticancer therapeutics, adjusting doses based on patient BSA does not reduce interpatient variablity in drug clearance [33]. This current study supported that claim, finding that BSA-based dosing regimen for LMP744 should not be utilized in clinical use. Though slight reductions were noticed in interpatient variations of clearance when normalized to BSA, these were not found to be statistically signicant. Weight was also found not to significantly alter the volume of distribution of LMP744, though a slight increase is seen in interpatient variation between volume of distribution and weight normalized volume of distribution values.

5.0 CONCLUSIONS AND FUTURE DIRECTIONS

The aim of this study was to support the clinical development of LMP744 by generating PK data via two different LC-MS/MS assays from plasma samples of 17 patients. The use of the novel, more sensitive, assay proved to be effective and sensitive enough to measure lower drug concentrations that the previously validated LC-MS/MS failed to measure. PK data analyzed using both noncompartmental and compartmental approaches. Noncompartmental $AUC_{0-\infty}$ was an underestimation of systemic plasma concentrations. Dose linearity could be suggested based on analysis of both C_{max} and AUC across all dose levels. Patient BSA had no significant effect on clearance and central volume of distribution was not significantly affected by weight.

Future directions from this study include continuing to analyze patient plasma samples provided from the dose escalation study. Additional samples will be used to update PK analyses and eventually explore the possible relationship between exposure and toxicity. Ultimately, if LMP744 is accepted as a candidate for phase 2 trials, determining the optimal dosage will mostly likely not depend on patient-specific BSA, but rather a fixed dose possibly derived from the results of this phase 1 dose escalation study.

BIBLIOGRAPHY

1. Champoux, J.J., *DNA Topoisomerases: Structure, Function, and Mechanism.* Annual Review of Biochemistry, 2001. **70**(1): p. 369-413.
2. Wang, J.C., *Cellular roles of DNA topoisomerases: a molecular perspective.* Nature Reviews Molecular Cell Biology, 2002. **3**(6): p. 430-440.
3. Seol, Y. and K.C. Neuman, *The dynamic interplay between DNA topoisomerases and DNA topology.* Biophysical reviews, 2016. **8**(Suppl 1): p. 101-111.
4. Pommier, Y., et al., *Roles of eukaryotic topoisomerases in transcription, replication and genomic stability.* Nat Rev Mol Cell Biol, 2016. **17**(11): p. 703-721.
5. Pommier, Y., *Topoisomerase I inhibitors: camptothecins and beyond.* Nat Rev Cancer, 2006. **6**(10): p. 789-802.
6. Hotte, S.J., et al., *Phase I trial of UCN-01 in combination with topotecan in patients with advanced solid cancers: a Princess Margaret Hospital Phase II Consortium study.* Ann Oncol, 2006. **17**(2): p. 334-40.
7. Romanelli, S., et al., *In vitro and in vivo interaction between cisplatin and topotecan in ovarian carcinoma systems.* Cancer Chemother Pharmacol, 1998. **41**(5): p. 385-90.
8. Crump, M., et al., *Phase I trial of sequential topotecan followed by etoposide in adults with myeloid leukemia: a National Cancer Institute of Canada Clinical Trials Group Study.* Leukemia, 1999. **13**(3): p. 343-7.
9. Schmidt, F., et al., *Topotecan-based combination chemotherapy for human malignant glioma.* Anticancer Res, 1999. **19**(2a): p. 1217-21.
10. Cao, S. and Y.M. Rustum, *Synergistic antitumor activity of irinotecan in combination with 5-fluorouracil in rats bearing advanced colorectal cancer: role of drug sequence and dose.* Cancer Res, 2000. **60**(14): p. 3717-21.
11. Wasserman, E., W. Sutherland, and E. Cvitkovic, *Irinotecan plus oxaliplatin: a promising combination for advanced colorectal cancer.* Clin Colorectal Cancer, 2001. **1**(3): p. 149-53.
12. Guichard, S., et al., *Combination of oxaliplatin and irinotecan on human colon cancer cell lines: activity in vitro and in vivo.* Anticancer Drugs, 2001. **12**(9): p. 741-51.
13. Covey, J.M., et al., *Protein-linked DNA Strand Breaks Induced in Mammalian Cells by Camptothecin, an Inhibitor of Topoisomerase I.* Cancer Research, 1989. **49**(18): p. 5016-5022.
14. Burke, T.G. and Z. Mi, *The structural basis of camptothecin interactions with human serum albumin: impact on drug stability.* Journal of Medicinal Chemistry, 1994. **37**(1): p. 40-46.
15. Staker, B.L., et al., *The mechanism of topoisomerase I poisoning by a camptothecin analog.* Proc Natl Acad Sci U S A, 2002. **99**(24): p. 15387-92.
16. Pommier, Y., *Drugging Topoisomerases: Lessons and Challenges.* ACS Chemical Biology, 2013. **8**(1): p. 82-95.

17. Antony, S., et al., *Novel indenoisoquinolines NSC 725776 and NSC 724998 produce persistent topoisomerase I cleavage complexes and overcome multidrug resistance.* Cancer Res, 2007. **67**(21): p. 10397-405.
18. Pommier, Y. and M. Cushman, *The indenoisoquinoline noncamptothecin topoisomerase I inhibitors: update and perspectives.* Mol Cancer Ther, 2009. **8**(5): p. 1008-14.
19. Kummar, S., et al., *Clinical and pharmacologic evaluation of two dosing schedules of indotecan (LMP400), a novel indenoisoquinoline, in patients with advanced solid tumors.* Cancer Chemother Pharmacol, 2016. **78**(1): p. 73-81.
20. Eisenblaetter, T., et al., *Dose Linearity and Proportionality*, in *Drug Discovery and Evaluation: Methods in Clinical Pharmacology*, F.J. Hock and M.R. Gralinski, Editors. 2011, Springer International Publishing: Cham. p. 695-714.
21. Le Tourneau, C., J.J. Lee, and L.L. Siu, *Dose escalation methods in phase I cancer clinical trials.* Journal of the National Cancer Institute, 2009. **101**(10): p. 708-720.
22. Administration, U.F.a.D., *Guidance for industry and Bioequivalence: Blood Level Bioequivalence Study*, FDA, Editor. 2016.
23. Antony, S., et al., *Cellular Topoisomerase I Inhibition and Antiproliferative Activity by MJ-III-65 (NSC 706744), an Indenoisoquinoline Topoisomerase I Poison.* Molecular Pharmacology, 2005. **67**(2): p. 523-530.
24. Hummel, J., et al., *Exploratory assessment of dose proportionality: review of current approaches and proposal for a practical criterion.* Pharm Stat, 2009. **8**(1): p. 38-49.
25. Sawyer, M. and M.J. Ratain, *Body surface area as a determinant of pharmacokinetics and drug dosing.* Invest New Drugs, 2001. **19**(2): p. 171-7.
26. Ratain, M.J., *Body-surface area as a basis for dosing of anticancer agents: science, myth, or habit?* J Clin Oncol, 1998. **16**(7): p. 2297-8.
27. Venditto, V.J. and E.E. Simanek, *Cancer therapies utilizing the camptothecins: a review of the in vivo literature.* Molecular pharmaceutics, 2010. **7**(2): p. 307-349.
28. Antony, S., et al., *Differential Induction of Topoisomerase I-DNA Cleavage Complexes by the Indenoisoquinoline MJ-III-65 (NSC 706744) and Camptothecin.* Base Sequence Analysis and Activity against Camptothecin- Resistant Topoisomerases I, 2003. **63**(21): p. 7428-7435.
29. Meng, L., Z.-Y. Liao, and Y. Pommier, *Non-Camptothecin DNA Topoisomerase I Inhibitors in Cancer Therapy.* Current topics in medicinal chemistry, 2003. **3**: p. 305-20.
30. Administration, U.F.a.D., *Guidance for Industry and Bioanalytical Method Validation* FDA, Editor. 2018.
31. Ito, S., *Pharmacokinetics 101.* Paediatrics & child health, 2011. **16**(9): p. 535-536.
32. Leon Shargel, e.a., *Drug Elimination and Hepatic Clearance* 6th ed. Applied Biopharmaceuitcs & Pharmacokinetics. 2012: McGraw-Hill.
33. Felici, A., J. Verweij, and A. Sparreboom, *Dosing strategies for anticancer drugs: the good, the bad and body-surface area.* Eur J Cancer, 2002. **38**(13): p. 1677-84.